

## **General Disclaimer**

### **One or more of the Following Statements may affect this Document**

- This document has been reproduced from the best copy furnished by the organizational source. It is being released in the interest of making available as much information as possible.
- This document may contain data, which exceeds the sheet parameters. It was furnished in this condition by the organizational source and is the best copy available.
- This document may contain tone-on-tone or color graphs, charts and/or pictures, which have been reproduced in black and white.
- This document is paginated as submitted by the original source.
- Portions of this document are not fully legible due to the historical nature of some of the material. However, it is the best reproduction available from the original submission.

**NASA TECHNICAL  
MEMORANDUM**

**NASA TM-78897**

NASA TM-78897

(NASA-TM-78897) A COMPARISON OF THE  
LUBRICATING MECHANISMS OF GRAPHITE FLUORIDE  
AND MOLYBDENUM DISULFIDE FILMS (NASA) 42 p  
HC A03/MF A01 C SCL 11H

N78-26215

G3/27 Unclas  
23338

A COMPARISON OF THE LUBRICATING MECHANISMS OF  
GRAPHITE FLUORIDE AND MOLYBDENUM DISULFIDE FILMS

by Robert L. Fusaro  
Lewis Research Center  
Cleveland, Ohio 44135

TECHNICAL PAPER to be presented at the  
Second International Conference on Solid Lubrication  
sponsored by the American Society of Lubrication Engineers  
Denver, Colorado, August 14-18, 1978



# A COMPARISON OF THE LUBRICATING MECHANISMS OF GRAPHITE FLUORIDE AND MOLYBDENUM DISULFIDE FILMS

Robert L. Fusaro  
National Aeronautics and Space Administration  
Lewis Research Center  
Cleveland, Ohio 44136

## Abstract

A microscopic study of 440C steel sliding surfaces lubricated by graphite fluoride or molybdenum disulfide solid lubricant rubbed films was conducted. The sliding surfaces, along with the friction, wear, and wear life were observed as a function of the number of sliding revolutions in three different atmospheres: moist air (10 000 ppm  $H_2O$ ), dry air (<20 ppm  $H_2O$ ), or dry argon (<20 ppm  $H_2O$ ). In general, the lubricating mechanisms of the two solid lubricants were found to be relatively similar; that is, a dynamic, thin, layer-like film (which sheared on relative motion) was formed between the two metallic surfaces. The mechanisms of failure were found to be somewhat different, however. Failure of  $MoS_2$  films was very dependent on atmospheric degradation, while that of graphite fluoride films was more dependent on flow of the lubricant film out of the contact zone.

## INTRODUCTION

Molybdenum disulfide ( $MoS_2$ ) is one of the most widely used solid lubricants. A considerable amount of research has been conducted on its friction properties and the reasons for its good lubricating behavior. Johnson (1), Winer (2), and Farr (3) have written excellent reviews on the history, the uses, and the fundamental knowledge of  $MoS_2$  as a lubricant.

Graphite fluoride ( $(CF_x)_n$ ) has been shown to have very good lubricating properties under various conditions and types of applications. Rubbed films of graphite fluoride have been shown to perform better than or equivalent to rubbed films of  $MoS_2$  or graphite in tests conducted on a pin-on-disk machine (4). These rubbed film results were further improved by bonding graphite fluoride to the surface using a polyimide (5) or an organopolysiloxane (6) polymer. In Ref. 7, good results were reported on epoxy phenolic or silicate bonded graphite fluoride films evaluated in a Failex machine.

Although many good lubricating results have been reported with graphite fluoride, poor results have also been reported (8, 9). The poor results were attributed to the abrasiveness (8) and the low load carrying capacity (8, 9) of graphite fluoride.

Most of the lubricating theories, the methods of evaluating, and the methods of applying and using solid lubricants have been based on studies of  $MoS_2$ . To date, very little research has been conducted on the fundamental lubricating mechanisms of graphite fluoride and how they compare to those of  $MoS_2$ . It might be that what is good for  $MoS_2$  is not good for graphite fluoride. Thus, the purpose of this investigation was to obtain a more fundamental understanding of how graphite fluoride lubricates and how failure occurs and to compare those findings

to how  $MoS_2$  lubricates and fails. The scope of this investigation included studying (1) how  $MoS_2$  and graphite fluoride films lubricate and the role of the transfer film in the lubrication process, and (2) how failure occurs, and the role of oxygen and  $H_2O$  in the failure process. To accomplish this, friction, wear rate of riders (which slid on both films), wear of the films, and wear lives were determined and compared for experiments conducted in atmospheres of moist air (10 000 ppm  $H_2O$ ), dry air (<20 ppm  $H_2O$ ), and dry argon (<20 ppm  $H_2O$ ).

A unique technique was used to study the lubrication and failure mechanisms, and that was to stop the tests at preset sliding intervals throughout the life of the films, and to examine the sliding surfaces by optical microscopy at high magnifications. The intent was to infer from the static surfaces what was occurring dynamically. The microscope was equipped with a vertical illuminator and two polarizing filters (one rotatable), thus the principles of light interference and birefringence of anisotropic crystals were used to study transfer, ordering, and the flow properties of the films.

The experimental conditions used were a pin-on-disk test apparatus, a test temperature of 25° C, a sliding speed of 2.6 meters per second (1000 rpm), and a load of 1 kilogram.

## MATERIALS

The graphite fluoride ( $(CF_x)_n$ ) used in this investigation had a fluorine to carbon ratio (as obtained from the manufacturer) of 0.85 to 1.00. A previous investigation (10) had shown that higher fluorine content graphite fluoride compounds do not give appreciably better lubrication results and they are considerably more difficult to make and more expensive to purchase. The average particle size of the graphite fluoride used was 10  $\mu m$ , but the size ranged from less than 1  $\mu m$  up to 30  $\mu m$ . The larger particles appeared to be conglomerations of the smaller particles, however.

The average particle size of the technical grade molybdenum disulfide ( $MoS_2$ ) used in this study was 10  $\mu m$ . The size ranged from less than 1  $\mu m$  to 75  $\mu m$ , and like graphite fluoride the larger particles appeared to be conglomerations of smaller particles.

The riders and disks were made of 440C HT tool steel and had a hardness of Rockwell C-60. The disks were lapped and polished to a surface finish of 0.09±0.02 CLA (centerline average) micrometers. The surfaces were then roughened by sanding in random directions with no. 150 grit wet sandpaper to a roughness of 0.30±0.05  $\mu m$  CLA.

The solid lubricant powders were applied to the roughened

surfaces by mechanically rubbing it over the surface at constant load (see Procedure Section). The thickness of the films obtained were found to be in the order of 1  $\mu\text{m}$  above the highest feature on the sanded metallic surface for the graphite fluoride film and about 2  $\mu\text{m}$  for the  $\text{MoS}_2$  film. Photomicrographs and surface profiles of the rubbed films are shown in Fig. 1.

## APPARATUS

A pin-on-disk type of sliding friction apparatus was used in this study. The apparatus used has been described in previous reports (4-9). Basically the friction specimens (fig. 2) consisted of a flat disk (6.3 cm diam) in sliding contact with a stationary hemispherically tipped rider (0.476 cm radius). The rider slid on a 5 cm diameter track on the disk, which gave it a linear sliding speed of 2.6 m/s at a disk rotation of 1000 rpm.

The apparatus used to apply the solid lubricant powder to the disks is shown in Fig. 3. The disk was attached to the vertical shaft of a small electric motor by use of a cup-shaped holder. Two vertical rods were used to restrain a floating metal plate to which was attached the solid lubricant applicators. In these experiments, the back of polishing cloths were used as applicators. The load was applied by placing weights on top of the metal plate.

The burnishing apparatus was designed to fit under the bell jar of a vacuum system, thus the atmosphere in which the films were applied could be controlled. This was done by pumping a vacuum and then backfilling with the desired atmosphere. Previous results (10, 11) have shown that films applied in moist air gave better friction and wear results than films applied in dry air, thus the films used in these experiments were applied in moist air.

## PROCEDURE

### Surface Cleaning

The cleaning procedure was as follows:

- (1) Scrub surfaces under running tap water with a brush to remove abrasive particles.
- (2) Clean surfaces with pure ethyl alcohol.
- (3) Rub surface with a water paste of levigated alumina. Clean until water readily wets surface.
- (4) Rinse under running tap water to remove levigated alumina (use brush to facilitate removal).
- (5) Rinse in distilled water.
- (6) Dry surfaces using dry compressed air. (Surfaces not dried quickly have a tendency to oxidize.)

### Film Application

The procedure for applying the rubbed films was as follows:

(1) Apply a small amount of solid lubricant powder to the cleaned disk surface and spread it evenly over the surface with the back of a polishing cloth.

(2) Apply about 1/2 gram of graphite fluoride (1 gram of  $\text{MoS}_2$ ) to the contact zone of the applicator (back of a polishing cloth attached to the floating metal plate) and distribute it evenly.

(3) Assemble apparatus as shown in Fig. 2 and apply two 1-kilogram weights as the applied load.

(4) Evacuate the bell jar and backfill it with a moist air atmosphere (10 000 ppm  $\text{H}_2\text{O}$ ). Continue to purge bell jar with moist air until application is complete.

(5) Set disk into rotation and gradually increase the speed to 15 rpm and rub for 1 hour.

(6) Remove disk from apparatus and blow off loose graphite fluoride or molybdenum disulfide loose debris from the surface using dry compressed air.

### Friction and Wear Tests

Insert rider and disk (with applied solid lubricant film) into the pin-on-disk apparatus and seal test chamber. Purge moist air through the chamber for 15 minutes prior to starting tests and continue to purge throughout test. After 15 minutes, set disk into rotation at 1000 rpm and gradually apply load. The test temperature was room temperature, approximately 25°C, and the load was 1 kilogram.

Each test was stopped at preset intervals of sliding. The rider and disk were removed from the friction apparatus and the contact areas were examined by optical microscopy and photographed. Surface profiles of the disk wear tracks were also taken. After examination, the rider and disk were reinserted into the apparatus and the previous test procedure repeated. The rider was not removed from the holder and locating pins in the apparatus insured that it was returned to its original position. Most tests were continued until failure occurred. The failure criterion was a friction coefficient of 0.30. Rider wear was calculated by measuring the diameter of the wear scar on the hemispherically tipped rider and then calculating the volume of material worn away.

### Analysis of Sliding Surfaces

Optical microscopy techniques were used to study the lubricating films, the transfer films, and the wear particles. The surfaces were viewed at magnifications to  $\times 1100$ . At these high magnifications, the vertical resolution was low (the order of 1  $\mu\text{m}$ ); this aspect was used to measure the heights of various features on the sliding surfaces, such as film thickness, wear track depth, etc.

Vertical illumination and observation of the surfaces allowed interference fringes to be seen in the films, both on the disk wear track and on the rider wear scar. Interference fringes indicated that the solid lubricant particles had flowed

together to form a continuous film that was very smooth and that the film was being sheared thinner and thinner in various areas. For example, the gradual depletion of the fringes in the inlet area of the rider wear scar, indicated that the films were thinner than the wavelength of light ( $0.4 \mu\text{m}$ ).

The microscope was also equipped with two polarizing filters (one which could be rotated); thus, the sliding surfaces were examined between crossed polarizing filters. The technique was especially useful with graphite fluoride since it was birefringent and the metallic wear debris was not. Thus this technique was used to distinguish graphite fluoride particles from metallic wear debris.

## RESULTS AND DISCUSSION

### Friction, Wear, and Wear Life

The friction, wear, and wear life results presented in this paper are typical of the various experimental conditions evaluated. All experiments were conducted at least twice and good repeatability was obtained. The purpose was to obtain a better understanding of the lubrication and failure mechanisms and how they were affected by atmosphere. Thus results presented were selected to show the trends rather than to define quantitative values.

Friction traces for 440C HT steel riders sliding on rubbed films of graphite fluoride ( $(\text{CF}_x)_n$ ) and molybdenum disulfide ( $\text{MoS}_2$ ) are shown in Fig. 4. Each film was evaluated at room temperature ( $25^\circ \text{C}$ ) in three different atmospheres; moist air of approximately 50 percent relative humidity (10 000 ppm  $\text{H}_2\text{O}$ ), dry air ( $<20$  ppm  $\text{H}_2\text{O}$ ), and dry argon ( $<20$  ppm  $\text{H}_2\text{O}$ ).

The friction coefficient and wear lives of  $\text{MoS}_2$  films were highly dependent on atmosphere. In dry air and dry argon, the friction coefficients were found to be nearly equal ( $<0.02$ ); however in moist air, the lowest value of friction coefficient obtained was 0.08. Wear life was more highly affected by atmosphere than was the friction coefficient. In moist air, failure occurred after only 10 kilocycles of sliding, while in dry air the wear life was 100 kilocycles and in dry argon it was 1800 kilocycles.

The friction coefficient of  $(\text{CF}_x)_n$  films was found to be very similar to  $\text{MoS}_2$  films, however the variation in wear life (in different atmospheres) was not as great. The longest wear life was obtained in moist air (380 kc) and the shortest in dry air (100 kc), dry argon gave an intermediate wear life of 180 kilocycles. An advantage of  $(\text{CF}_x)_n$  over  $\text{MoS}_2$  is its ability to lubricate for longer periods of time (380 vs. 10 kc) under environmental conditions which one might consider normal (50 percent relative humidity air). Under inert conditions however  $\text{MoS}_2$  was superior to  $(\text{CF}_x)_n$ .

Rider wear as a function of sliding duration is shown in Fig. 5 for riders which slid on the  $\text{MoS}_2$  films and  $(\text{CF}_x)_n$  films in the three different atmospheres. In dry air and dry argon less rider wear occurred for the riders which slid on

$\text{MoS}_2$  films than on  $(\text{CF}_x)_n$  films, however in moist air the opposite was true. In general, rider wear did not increase at a constant rate. There appeared to be three regimes to the wear process; the first was an interval of high but gradually decreasing wear rate, the second was an interval of relatively constant wear rate, and the third was an interval of gradually increasing wear rate.

These regimes can be more easily seen in Table I, where rider wear rate (wear volume per unit sliding distance) is given for each sliding interval used in this investigation. The first rider wear regime (which might be considered "run-in") was markedly affected by water vapor in the air atmosphere for both solid lubricants. Rider wear rates were from 4 to 10 times higher in moist air than in the dry atmospheres. The rider wear rate on the  $\text{MoS}_2$  film in moist air was found to be high in all three regimes; however, after "run-in" the rider wear rate on the  $(\text{CF}_x)_n$  film in moist air was found to be similar to that found in the dry atmospheres. In dry air, similar rider wear rates were obtained on both  $\text{MoS}_2$  films and  $(\text{CF}_x)_n$  films; however in an inert atmosphere (dry argon) lower rider wear rates (for a considerably longer period of time) were obtained on  $\text{MoS}_2$  films than  $(\text{CF}_x)_n$  films.

### $\text{MoS}_2$ LUBRICATION AND FAILURE MECHANISMS

The method used to study lubrication and failure mechanisms in this study was to stop the tests at preset sliding intervals, and examine the sliding surfaces by optical microscopy at high magnifications. Thus the tests were stopped and the surfaces examined after sliding durations of 1, 5, 15, 60, 100, 200, 400, 700, and 1500 kilocycles; or at failure (a friction coefficient of 0.30). The results obtained were very dependent on the atmosphere in which the  $\text{MoS}_2$  films were evaluated, thus each atmosphere will be presented separately.

#### Moist Air

The first atmosphere to be discussed is an atmosphere which might be considered a typical condition; that is, an atmosphere of 50 percent relative humidity air at  $25^\circ \text{C}$  (10 000 ppm  $\text{H}_2\text{O}$ ). Figure 6 shows the sliding surfaces after 1, 5, and 10 kilocycles of sliding.

After only 1 minute of sliding (fig. 6(a)), a large buildup of  $\text{MoS}_2$  is seen in the entrance region of the scar. The  $\text{MoS}_2$  is powdery at the leading edge, but it becomes highly compressed towards the contact region. In fact, in the contact region, the  $\text{MoS}_2$  particles coalesce and it is impossible to distinguish individual particles. The coalesced  $\text{MoS}_2$  film tends to plastically flow across the contact area and then break up into fine powdery material in the exit. Coalescing and plastic flow seem to be characteristics that good solid lubricants possess. Sliney (12) has observed this with an optical microscope by viewing dynamically various solid lubricant powders, as they pass through the contact area of a metal ball sliding on a glass disk.

The wear track on the rubbed  $\text{MoS}_2$  films is shown in

Fig. 6(a) and 7(a) after 1 kilocycle of sliding. In the center of the wear track most of the original film has been plowed away and what remained was compacted  $\text{MoS}_2$  in the sanded scratches. The  $\text{MoS}_2$  tended to flow from the scratches in very thin films across the flat metallic plateaus between the scratches.

Figure 6(b) shows the sliding surfaces after 5 kilocycles of sliding. A definite change on the sliding surfaces has taken place; most of the smooth, condensed material is gone and what remains is black powdery debris. The high magnification photomicrographs of Fig. 7(b) show areas within the condensed  $\text{MoS}_2$  films which are transforming to a black, powdery material.

After 10 kilocycles of sliding, failure occurred (a friction coefficient of 0.30). Figure 6(c) shows the sliding surfaces after failure. No smooth, condensed  $\text{MoS}_2$  films were found on either the rider or the wear track. Instead, a heavy, rippled powdery film was found on both rider and disk sliding surfaces (fig. 7(c)). It is interesting to note that failure was marked by the buildup of a heavy transfer film on both surfaces and that no galling was evident on either surface.

#### Dry Air

The chemical decomposition of  $\text{MoS}_2$  films under sliding conditions has been the subject of several studies (13-19). It has been shown that the most predominant chemical reaction taking place is the oxidation of  $\text{MoS}_2$ . It has also been proposed that  $\text{H}_2\text{O}$  in the atmosphere greatly accelerates the oxidation process (17). To determine the effect of water vapor on the lubrication and failure mechanisms of  $\text{MoS}_2$  films, similar experiments to those in moist air were conducted in dry air ( $<20$  ppm  $\text{H}_2\text{O}$ ).

Figure 8 gives photomicrographs of the sliding surfaces in dry air after 1 kilocycle of sliding. Transfer to the rider at this point (fig. 8(a)) is seen to be similar to that found in moist air (fig. 6(a)), that is the transfer was fairly heavy. On continued sliding, however, the transfer film became very thin. This type of transfer was not observed in moist air, but it did occur in dry argon; thus discussion of this type of transfer will be deferred until the Dry Argon section. At failure, transfer looked very similar to that found in moist air (fig. 6(c)), that is a heavy, rippled, coarser type of transfer film occurred.

The  $\text{MoS}_2$  film on the wear track after 1 kilocycle of sliding (fig. 8(b)) more continuously covered the surface and had more of a metallic luster than did the wear track films formed in moist air (fig. 6(b)). After 5 kilocycles of sliding, transformation of the metallic colored  $\text{MoS}_2$  films to blackish colored areas was found to occur (fig. 9(a)), and as sliding continued the number and size of these areas increased (fig. 9(b)). In areas where the film was thicker, the black areas took the form of bubbles (fig. 9(a) and (b)). At failure (100 kc of sliding), a powdery buildup of material like that found in moist air was found on the wear track (fig. 7(c)). Thus it was

observed that the transformation of  $\text{MoS}_2$  occurred in dry air as well as moist air, however the rate was much slower in dry air.

#### Dry Argon

The bubbles observed on the film wear track in dry air were very similar to what Salomon, DeGee, and Zaat have found in previous studies (15, 16), and to which they have attributed to oxidation of  $\text{MoS}_2$ . To determine the effect of oxidation on the lubrication and failure mechanisms of rubbed  $\text{MoS}_2$  films, similar experiments to those conducted in dry and moist air were conducted in dry argon ( $<20$  ppm  $\text{H}_2\text{O}$ ) at  $25^\circ\text{C}$ .

Figure 10 gives high magnification photomicrographs of interesting features found on the film wear track after various sliding intervals in dry argon. After 1 kilocycle of sliding (fig. 11(a)), the film on the wear track was smooth and continuous and the metallic substrate could not be seen. A few bubble-like protrusions could be seen after 1 kilocycle of sliding at the outer edges of the wear track (fig. 10(a)), and after longer durations of sliding these bubbles could be found also in the center of the wear track. Figure 10(b) shows one of these bubble areas in which the bubbles have cracked and spalled from the surface. These areas of bubbling, cracking, and spalling were localized and most of the track remained smooth and continuous. Since no change occurred in color (i.e., they remained metallic colored and did not turn black), it is surmised that no transformation of  $\text{MoS}_2$  was occurring.

On continued sliding, the spalled areas tended to be self-healing; nevertheless, after long sliding durations (700 kc) the films started to thin in the center (fig. 10(c)). At failure (1860 kc of sliding), the wear track surface was covered with a coarse, powdery type of material. Thus, as found in moist air and dry air, failure was characterized by the buildup of a coarse, powdery film. In contrast to the air results though, this powdery debris was believed to result from the depletion of  $\text{MoS}_2$  by the radial flow from the contact area rather than by depletion of  $\text{MoS}_2$  by chemical transformation.

Transfer films to the rider are shown after 1 and 400 kilocycles of sliding in Fig. 11. After 1 kilocycle of sliding, transfer was not markedly different than that found for tests in moist and dry air, except that the transfer tended to flow more through the central portion of the scar and there was less buildup at the edges of the rider scar. As sliding continued the transfer on the rider scar became thinner and thinner. Figure 12(b) shows the transfer after 400 kilocycles of sliding. The  $\text{MoS}_2$  tended to buildup in the rider entrance and then was sheared extremely thin as it passed through the contact area. Transfer films similar to this were found in dry air; but not in moist air, because of the rapid degradation of the  $\text{MoS}_2$ . Similarly to dry and moist air, at failure heavy, coarse transfer was found.

#### Graphite Fluoride Lubrication and Failure Mechanisms

Experiments identical to those conducted on  $\text{MoS}_2$  films

were also performed on graphite fluoride ( $(CF_x)_n$ ) films. Since  $(CF_x)_n$  was transparent to light and double refracting, the principles of light interference and birefringency were used to analyze the films and determine if  $(CF_x)_n$  was present.

#### Moist Air

Photomicrographs of a rider wear scar and a wear track on a  $(CF_x)_n$  film are shown in Fig. 12 after 1 kilocycle of sliding in a moist air atmosphere. In contrast to the  $MoS_2$  results, no heavy transfer film was found on the rider wear scar. The  $(CF_x)_n$  tended to build up in the inlet region and then thin as it approached the contact region. Figure 12(a) shows interference fringes which gradually disappear into a milky colored region on the rider scar. This indicated the  $(CF_x)_n$  film was sheared too thin for interference fringes to occur. In a few instances, thicker sheared particles of  $(CF_x)_n$  pass through the contact region (as seen in fig. 12(a)), but for the most part the thickness of the transfer was less than the wavelength of light (about  $4 \times 10^{-7}$  in).

The wear track on the disk was characterized by highly colored interference bands (fig. 12(b)). The  $(CF_x)_n$  readily flowed over both surfaces and produced films on the wear track which were in the order of  $4 \times 10^{-7}$  to  $8 \times 10^{-7}$  meters thick (the wavelength of light). The good flow properties were detrimental in one aspect, however, and that was  $(CF_x)_n$  also tended to flow out of the contact area. Figure 12(b) shows the flow as a buildup at the sides of the wear track and as birefringent debris further from the track. This along with the fact that the  $(CF_x)_n$  tended to pop out or spall from some of the scratches (fig. 12(b)) was deemed the major cause of failure in these experiments.

As a general rule, failure of the  $(CF_x)_n$  films was not abrupt, but a gradual process. After run-in, a period of relatively constant friction occurred which was followed by a period of gradually increasing friction. During the constant friction phase, the film was gradually being depleted. Figure 13 shows the depletion of the film after 100 kilocycles of sliding. A considerable amount of  $(CF_x)_n$  was still present on the wear track, but the film on the nonscratched areas was not nearly as prevalent.

Even though the film on the wear track was being depleted, the rider wear scar after 100 kilocycles did not look much different than it did after 1 kilocycle of sliding. The major difference is that the scar was larger and that there was less  $(CF_x)_n$  in the inlet area. The transfer film on the rider looked about the same, with the exception that some birefringent  $(CF_x)_n$  transfer was present.

What happened to the surfaces when friction was gradually increasing was quite interesting. Figure 14 shows the surfaces at the time the friction coefficient reached a value of 0.20 (308 kc of sliding). Dark bands of heavy transfer were seen on both the rider wear scar and the film wear track. These bands were found to be a mixture of  $(CF_x)_n$  and fine metallic wear particles. The formation of these bands was

believed to result from the depletion of  $(CF_x)_n$  from localized regions in the film wear track. These regions generate excessive metallic wear particles which mix with  $(CF_x)_n$  present in other regions to produce circumferential bands on the track.

High magnification observation of these bands indicated that even though they contained fine metallic debris, flow still occurred (fig. 14). After 380 kilocycles of sliding, however, the flow properties of the film (both on the rider and the disk wear track) were not nearly as good. Transfer became darker and more powdery. Examination of the wear areas under crossed polarizing filters, showed very few birefringent particles.

#### Dry Air

$(CF_x)_n$  films were also evaluated in a dry air atmosphere. In dry air the same three regimes of friction occurred. A run-in phase ( $\mu = 0.10$ ), a low friction phase ( $\mu = 0.02$ ), and a phase of gradually increasing friction. The tests were stopped and the surfaces were observed in each of the three regimes. Figure 16 gives photomicrographs of the same area on the  $(CF_x)_n$  film wear track taken during the (a) "run-in" phase (1/4 kc of sliding), (b) during the low friction phase (3 kc of sliding), and (c) during the high friction phase (24 kc of sliding).

In general, there was not a great deal of difference in appearance between the surfaces evaluated in dry air and in moist air. "Run-in" consisted of plastically deforming the  $(CF_x)_n$  particles into a smooth, coalesced, thin film and the wearing off of any metallic asperities that protruded through the film. The low or constant friction phase consisted of sliding on these coalesced films, and the higher friction phase consisted of the gradual depletion of  $(CF_x)_n$ .

One obvious difference in surface characteristics between moist air and dry air was that in dry air the  $(CF_x)_n$  disengaged from the scratches much more readily than it did in moist air. This disengagement can be seen in Fig. 15(b) and (c), where empty scratches can be seen. Another difference is that during the low friction phase, the  $(CF_x)_n$  in dry air tended to clump together more than it did during the moist air tests (fig. 15(b)). It is possible that disengagement from the scratches was in some way related to the lower friction obtained, but it was also detrimental to wear life due to the fact that it led to a more rapid depletion of  $(CF_x)_n$  from the wear track.

Figure 16 shows photomicrographs of the rider transfer films which correspond to the intervals of Fig. 15. Compared to the moist air tests, the rider run in dry air had a thicker transfer film on it. Also there was more transferred  $(CF_x)_n$  material at the sides of the wear scar than found for moist air tests. The difference in transfer may have been a contributing factor to the lower friction attained in dry air.

In Fig. 16(c) very fine metal particles can be seen in the entrance region of the rider. The rider transfer film in the contact region of the same photograph appears to be "heavier"

and not as smooth as in the previous two photographs. Most likely this transfer is also a combination of  $(CF_x)_n$  and metallic particles.

#### Dry Argon

The results from tests which were conducted in a dry argon atmosphere were very similar to those obtained in dry air. Rider wear scars, transfer films, and the  $(CF_x)_n$  film near tracks did not look much different. Figure 17 gives photomicrographs of the film wear track after (a) 1, (b) 15, (c) 60, and (d) 180 kilocycles of sliding. The same general film wear process (as was found in moist air or in dry air) was found to also occur in dry argon, and that was a gradual depletion of the  $(CF_x)_n$  from the contact region.

One difference between the dry air and dry argon tests was that the  $(CF_x)_n$  did not as readily disengage from the scratches, and this most likely was the reason for the longer life in dry argon. Another difference was that heavy bands of transfer did not form on the surface of the rider or the disk wear track when high friction occurred as it did in moist air and in dry air. Some disengagement from the scratches did occur in the form of small bubbles as can be seen in Fig. 17(b).

#### Comparison of $MoS_2$ and $CF_x$

Both  $MoS_2$  and  $(CF_x)_n$  were found to form transfer films and to flow plastically in the contact region. Transfer film formation was found to be of a dynamic nature. Solid lubricant built up in the rider scar entrance region and was gradually fed into the contact region, where it sheared and gradually flowed to the exit.

On both  $MoS_2$  and  $(CF_x)_n$  rubbed films, a very thin, smooth, coalesced film of each solid lubricant was produced by the rider during the initial stages of sliding. The thickness of the film produced was found to be greater for  $MoS_2$  than for  $(CF_x)_n$ . The thickness of the  $(CF_x)_n$  film produced was in the order of the wavelength of light (0.4 to 0.8  $\mu m$ ) while the thickness of the  $MoS_2$  film produced was in the order of 1  $\mu m$ . As sliding continued, the films tended to get thinner due to radial flow (or transverse flow) from the contact. Thus the scratches on the surface served two purposes and that was they tended to restrict the radial flow of the lubricant and they served as a reservoir.

The mechanical stresses of sliding, also induced bubbles and bulges to occur in localized areas of the film wear track, which caused cracking and spalling to occur. As long as plentiful supply of lubricant was available on the film wear track, the films healed. However, during this process a certain amount of lubricant found its way out of the contact region which also resulted in thinning of the films.

The major difference between the lubricating mechanisms of the two solid lubricants, was that failure of  $MoS_2$  films was much more dependent upon atmospheric conditions than were  $(CF_x)_n$  films. In air (and especially moist air), the mechani-

cal stresses of sliding induced the transformation of bright, metallic colored films of  $MoS_2$  to black, powdery looking  $MoS_2$  films, with the result that the wear lives were shortened considerably. The wear lives of  $(CF_x)_n$  were also affected by atmosphere, but to a lesser extent than  $MoS_2$  films.

Optical observation of the  $(CF_x)_n$  films at high magnifications did not indicate that transformation of  $(CF_x)_n$  was taking place. However, Atkinson and Waghorne (20) have studied failed surfaces of graphite fluoride films by X-ray photoelectron spectroscopy and deduced that failure was due to the chemical decomposition of the graphite fluoride. They give no details about the friction and wear tests or the condition of the surfaces, thus it is hard to compare those results to this study. If decomposition of  $(CF_x)_n$  occurred in this study, there was no optical evidence that any decomposition product was harmful to the lubrication process.

#### SUMMARY OF RESULTS

Friction, wear, and optical microscopy studies of molybdenum disulfide ( $MoS_2$ ) and graphite fluoride ( $(CF_x)_n$ ) (rubbed films in moist air (10 000 ppm  $H_2O$ ), dry air (<20 ppm  $H_2O$ ), and dry argon (<20 ppm  $H_2O$ ) atmospheres indicated that:

1. The lubricating mechanisms of the two solid lubricants were relatively similar. The mechanism consisted of the formation of a thin, coalesced solid lubricant film on each sliding surface during the initial stages of sliding, and then the continual plastic flow (shear) of this film between the sliding surfaces. Transfer film formation was found to be of a "dynamic" nature. The solid lubricant powder built up in the entrance region of the rider scar, became compacted, and eventually coalesced into a very thin film in the contact region as it flowed towards the exit region.

2. Two failure mechanisms were found to be operating. The first, which was more prevalent with  $MoS_2$  than with  $(CF_x)_n$  was believed to be due to chemical decomposition. In air, bright, metallic colored, coalesced films of  $MoS_2$  were observed to transform to a blackish more powdery type of material, but in dry argon this did not occur. The second failure mechanism was due to the gradual depletion of the films by radial flow (or transverse flow) or by cracking and spalling of the films.

3. Graphite fluoride tended to flow from the contact area more readily than did  $MoS_2$ ; thus the scratches on the surface (to which the solid lubricant was applied) served two purposes with  $(CF_x)_n$  (also to a lesser extent with  $MoS_2$ ) and that was they tended to restrict the outward flow of the  $(CF_x)_n$  and they served as a reservoir for the solid lubricant.

#### REFERENCES

1. Johnson, R. L., "A Review of the Early Use of Molybdenum Disulfide as a Lubricant," NASA TM X-52343, 1967.
2. Winer, W. O., "Molybdenum Disulfide as a Lubricant: A Review of the Fundamental Knowledge," Wear, 10, 422-452 (1965).



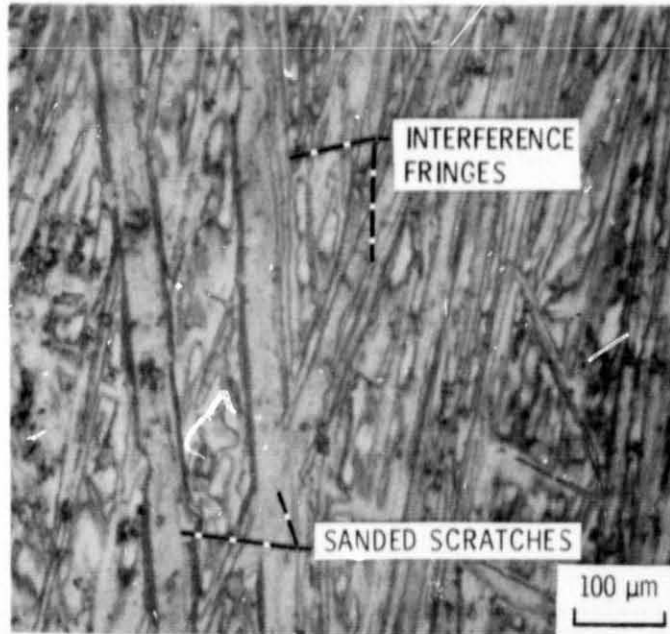
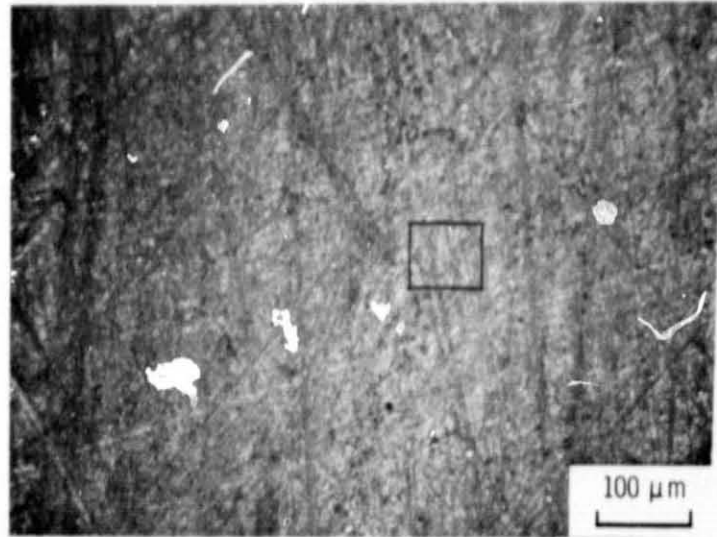
3. Farr, J. P. G., "Molybdenum Disulphite in Lubrication. A Review," Wear, 35, 1-22 (1975).
4. Fusaro, R. L., and Sliney, H. E., "Graphite Fluoride (CF<sub>x</sub>)<sub>n</sub> -- A New Solid Lubricant," ASLE Trans., 13, 56-66 (1970).
5. Fusaro, R. L., and Sliney, H. E., "Graphite Fluoride as a Solid Lubricant in a Polyimide Binder," NASA TN D-6714, 1972.
6. Fusaro, R. L., "Organopolysiloxane-Bonded Graphite Fluoride as a Solid Lubricant," NASA TN D-8033, 1975.
7. Glasser, H., Petronio, M., and Shapiro, A., "Graphite Fluoride as a Solid Lubricant," Lubr. Eng., 28, 161-164 (1972).
8. McConnell, B. D., Snyder, C. E., and Strang, J. R., "Analytical Evaluation of Graphite Fluoride and Its Lubrication Performance under Heavy Loads," Lubr. Eng., 33, 184-190 (1977).
9. Mechlenburg, K. R., "The Effect of Wear on the Compressive Stress in the Sphere-on-Plane Configuration," ASLE Trans., 17, 149-157 (1974).
10. Peterson, M. B. and Johnson, R. L., "Friction and Wear Investigation of Molybdenum Disulfide I - Effect of Moisture," NACA TN-3055, 1953.
11. Fusaro, R. L., "Graphite Fluoride Lubrication: The Effect of Fluorine Content, Atmosphere, and Burnishing Technique," ASLE Trans., 20 (1), 15-24 (1977).
12. Johnston, R. R. M., and Moor, A. J. W., "The Burnishing of Molybdenum Disulphide onto Metal Surfaces," Wear, 7, 498-512 (1964).
13. Sliney, H. E., "Dynamics of Solid Lubrication as Observed by Optical Microscopy," ASLE Preprint No. 76-LC-1B-4, Presented at ASLE/ASME Lub. Conf., Boston, MA, Oct. 5-7, 1976.
14. Ross, S., and Sussman, A., "Surface Oxidation of Molybdenum Disulfide," J. Phys. Chem., 59, 889-892 (1955).
15. Haltner, A. J., and Oliver, C. S., "Effect of Water Vapor on the Friction of Molybdenum Disulfide," Ind. Eng. Chem. Fundam., 5, 348-355 (1966).
16. Salomon, G., De Gee, A. W. J., and Zaat, J. H., "Mechano-Chemical Factors in MoS<sub>2</sub> Film Lubrication," Wear, 7, 87-101 (1964).
17. De Gee, A. W. J., Salomon, G., and Zaat, J. H., "On the Mechanisms of MoS<sub>2</sub> Film Failure in Sliding Friction," ASLE Trans., 8, 156-162 (1965).
18. Pritchard, C., and Midgley, J. W., "The Effect of Humidity on the Friction and Life of Unbonded Molybdenum Disulphide Films," Wear, 13, 39-50 (1969).
19. Pardeo, R. P., "The Effect of Humidity on Low-Load Frictional Properties of a Bonded Solid Film Lubricant," ASLE Trans., 15, 130-142 (1972).
20. Gansheimer, J., "A Review on Chemical Reactions of Solid Lubricants during Friction," ASLE Trans., 15 (4), 244-251 (1972).
21. Atkinson, I. B., and Waghorne, R. M., "Tribo-Chemistry of Graphite Fluoride Studied Using X-Ray Photoelectron Spectroscopy," Wear, 37, 123-128 (1976).

TABLE I. - EFFECT OF ATMOSPHERE ON THE RIDER WEAR RATE FOR RIDERS WHICH SLID ON RUBBED FILMS OF GRAPHITE FLUORIDE OR MOLYBDENUM DISULFIDE

Sliding Interval, kc	Rider wear rate (m <sup>3</sup> /m <sup>2</sup> ×10 <sup>-15</sup> )					
	Moist air (10 000 ppm H <sub>2</sub> O)		Dry air (<20 ppm H <sub>2</sub> O)		Dry argon (<20 ppm H <sub>2</sub> O)	
	MoS <sub>2</sub>	(CF <sub>x</sub> ) <sub>n</sub>	MoS <sub>2</sub>	(CF <sub>x</sub> ) <sub>n</sub>	MoS <sub>2</sub>	(CF <sub>x</sub> ) <sub>n</sub>
0 - 1	2.0	1.59	0.19	0.44	0.17	0.45
1 - 5	.65	.43	.045	.088	.041	.058
5 - 15	----	.030	.056	.068	----	.029
5 - 10	2.4	----	----	----	----	----
15 - 60	----	.040	.077	.17	.012	.025
60 - 100	----	.11	.16	<sup>a</sup> .28	.012	.025
100 - 200	----	.12	----	----	----	<sup>b</sup> .52
200 - 1500	----	<sup>c</sup> .45	----	----	.012	----
1500 - 1800	----	----	----	----	.018	----

<sup>a</sup>60 - 90 kc.  
<sup>b</sup>100 - 180 kc.  
<sup>c</sup>200 - 308 kc.

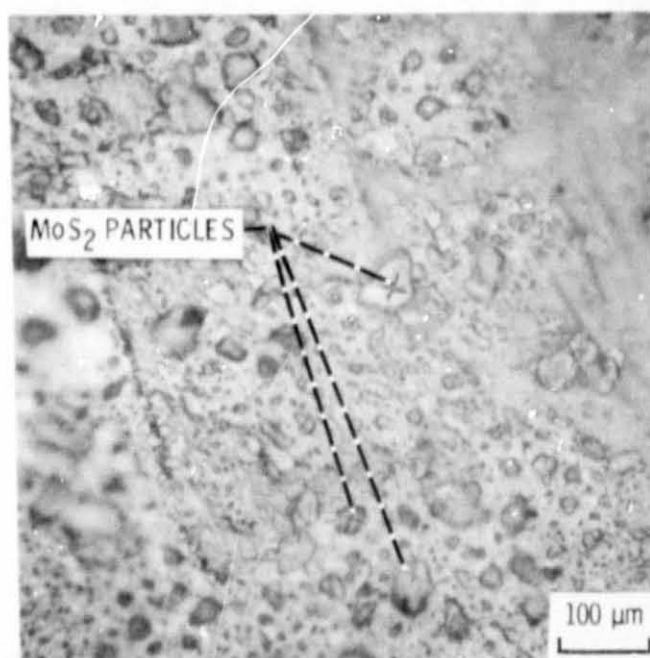
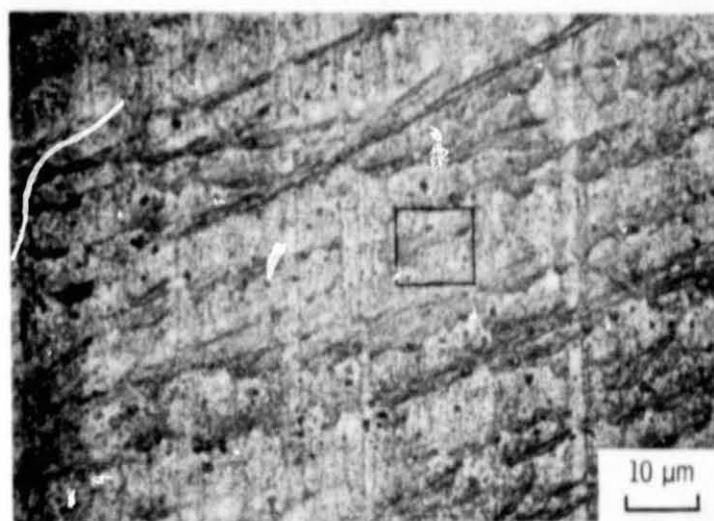
E-9633



(a) GRAPHITE FLUORIDE RUBBED FILM.

Figure 1. - Photomicrographs and surface profiles before friction and wear test were performed.

ORIGINAL. PAGE IS  
OF POOR QUALITY



(b) MOLYBDENUM DISULFIDE RUBBED FILM.

Figure 1. - Concluded.

ORIGINAL PAGE IS  
OF POOR QUALITY

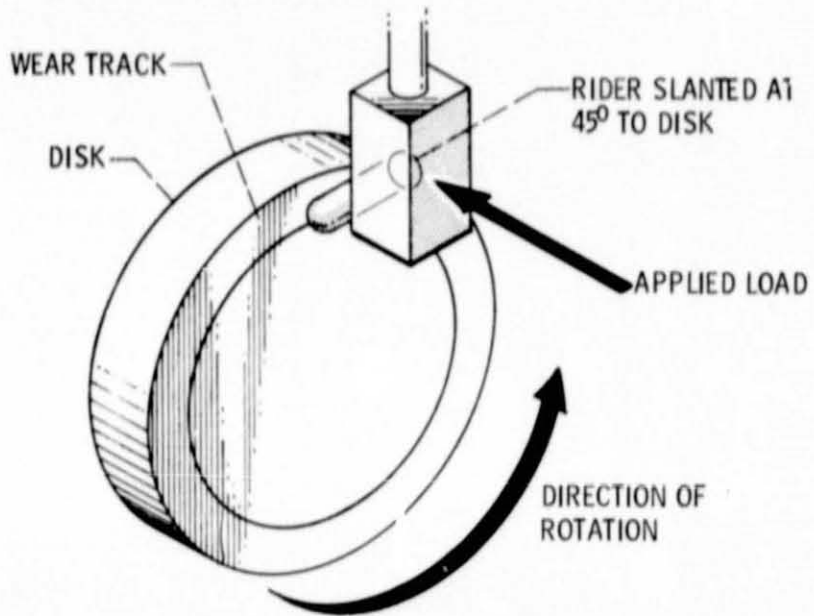


Figure 2. - Schematic diagram of friction apparatus.

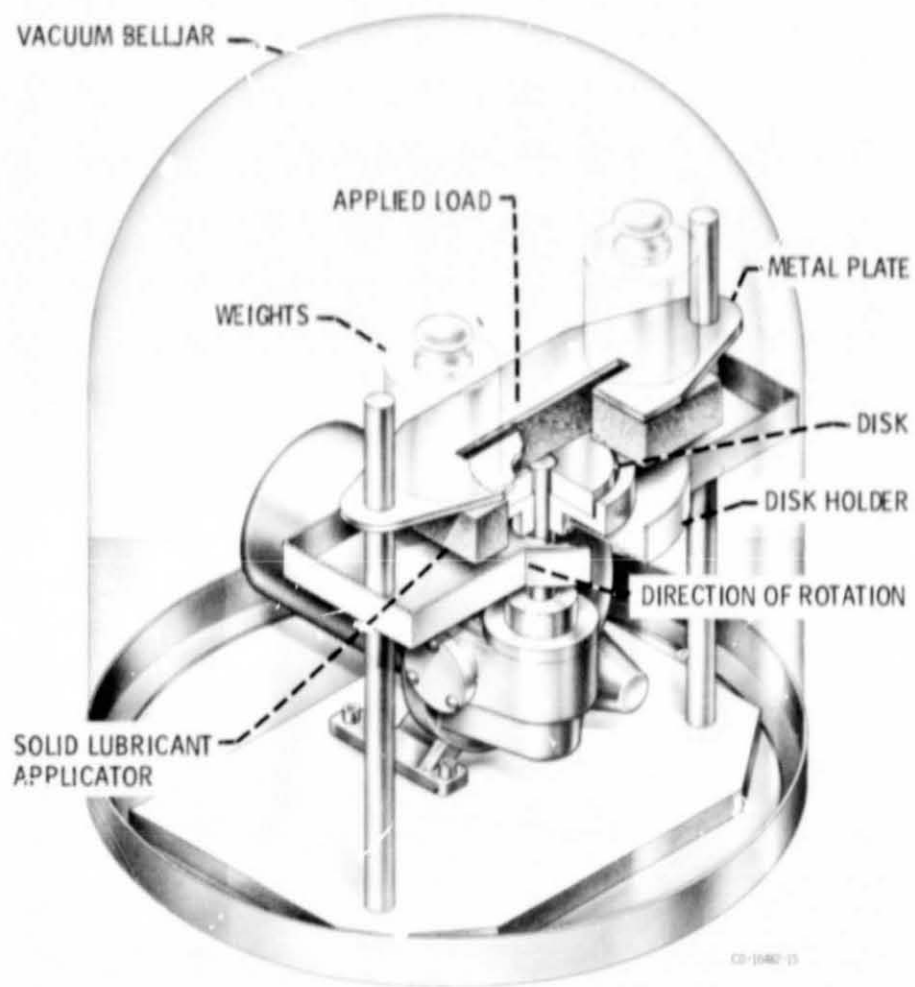


Figure 3. - Apparatus used for applying  $\text{MoS}_2$  and  $(\text{CF}_x)_n$ .

ORIGINAL PAGE IS  
OF POOR QUALITY

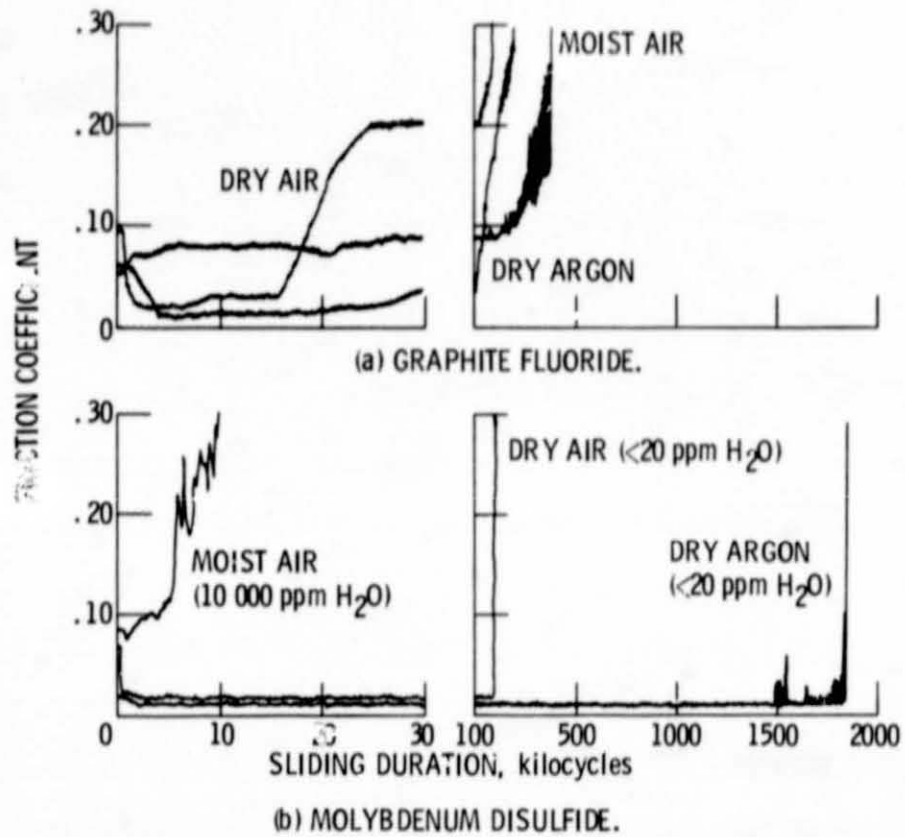


Figure 4. - Friction coefficient as a function of sliding duration for (a) Graphite fluoride films and (b) Molybdenum disulfide films evaluated in three different atmospheres.

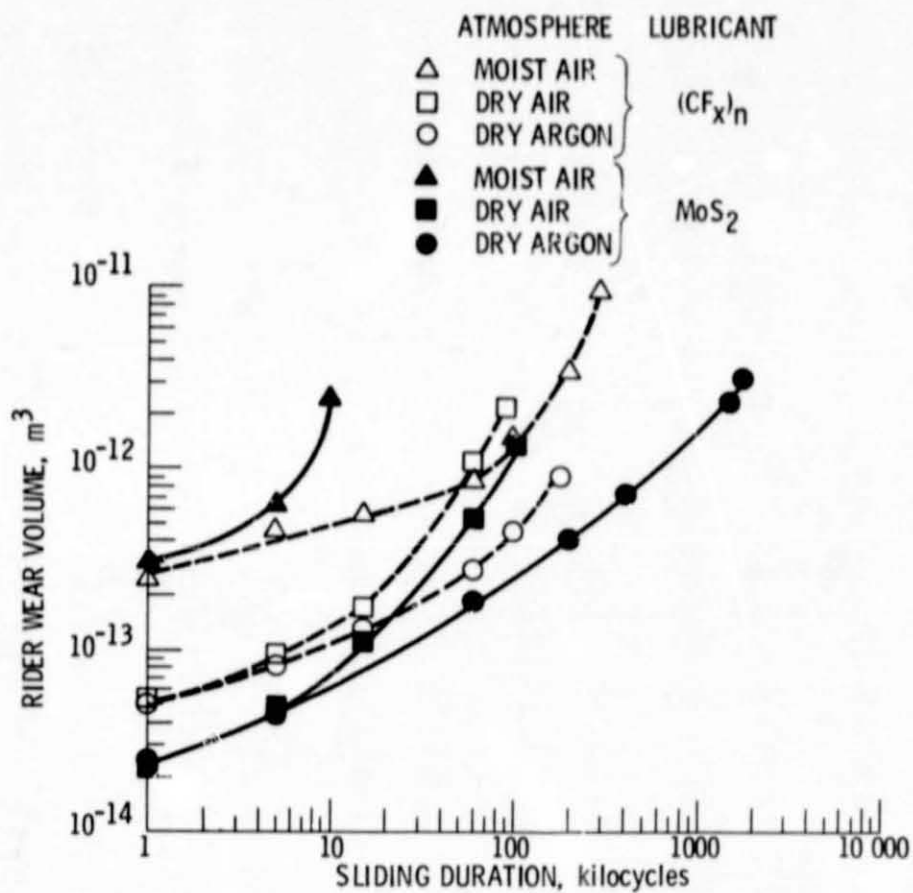
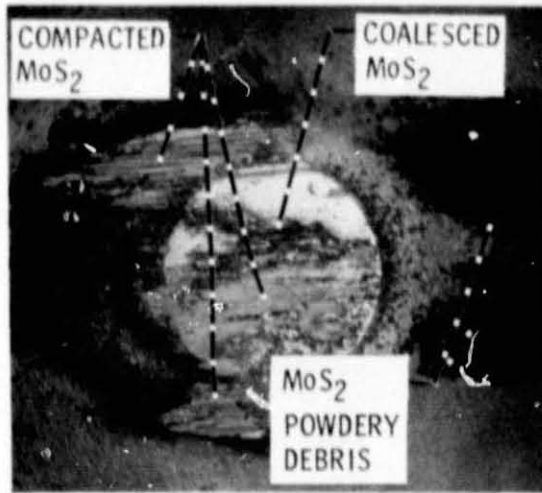


Figure 5. - Effect of atmosphere on rider wear volume as a function of sliding duration for riders which slid on graphite fluoride or molybdenum disulfide films rubbed onto sanded 440C HT steel disks.

ORIGINAL PAGE #  
OF POOR QUALITY



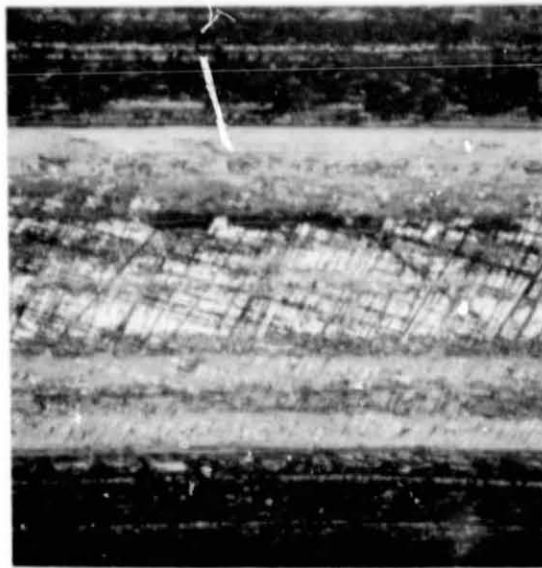
(a) 1 kc OF SLIDING.

Figure 6. - Photomicrograph of rider wear scars and MoS<sub>2</sub> film wear tracks taken after various sliding intervals in a moist air atmosphere (10,000 ppm H<sub>2</sub>O).

ORIGINAL PAGE #  
OF POOR QUALITY

E-9533



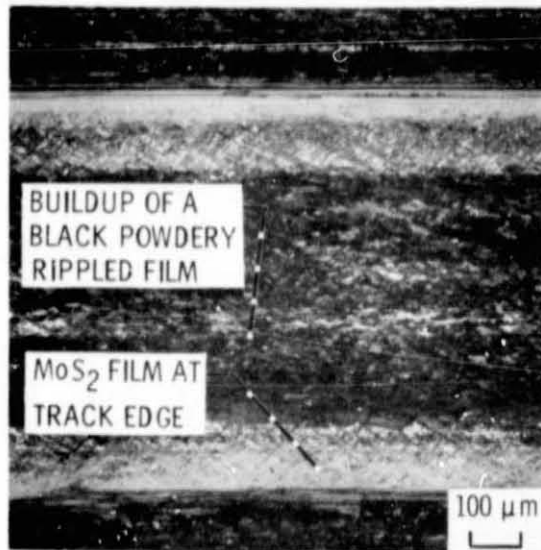
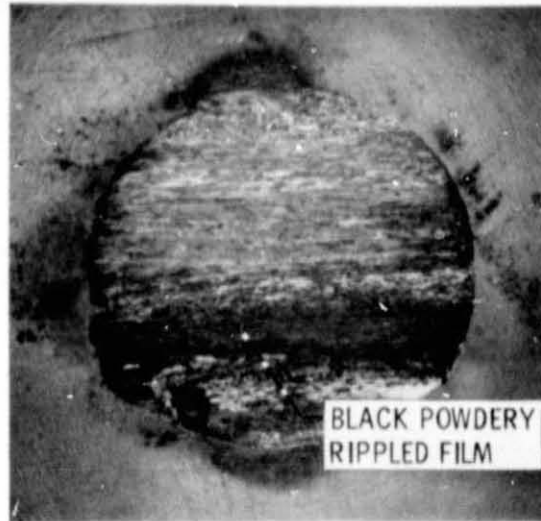


(b) 5 kc OF SLIDING.

Figure 6. - Continued.

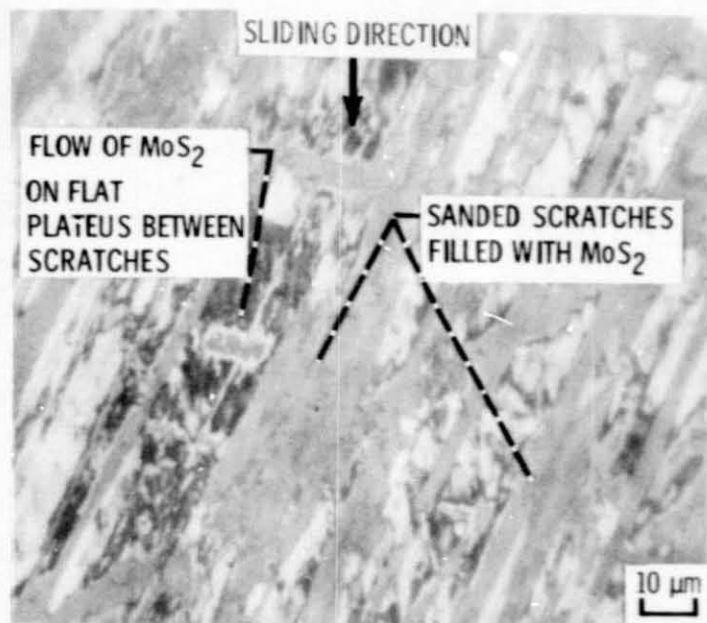
ORIGINAL PAGE IS  
OF POOR QUALITY

E-9533

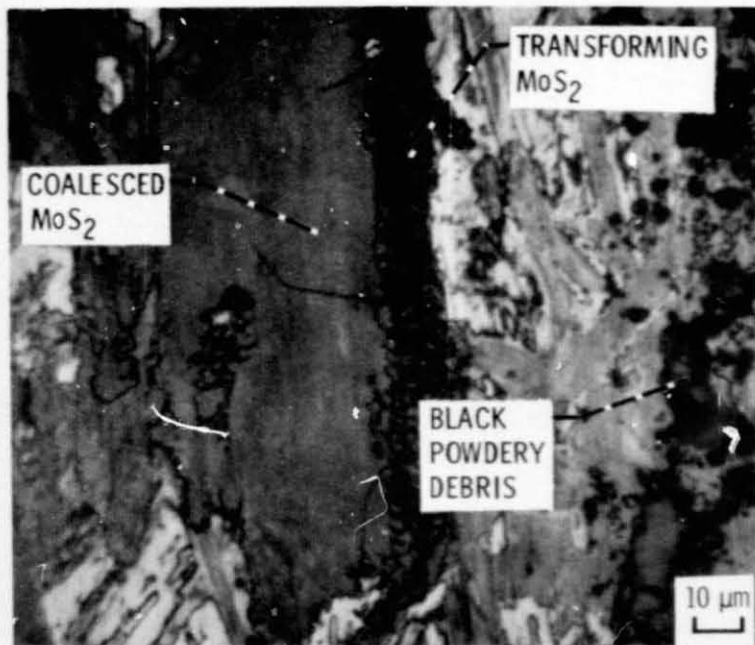


(c) 10 kc OF SLIDING.

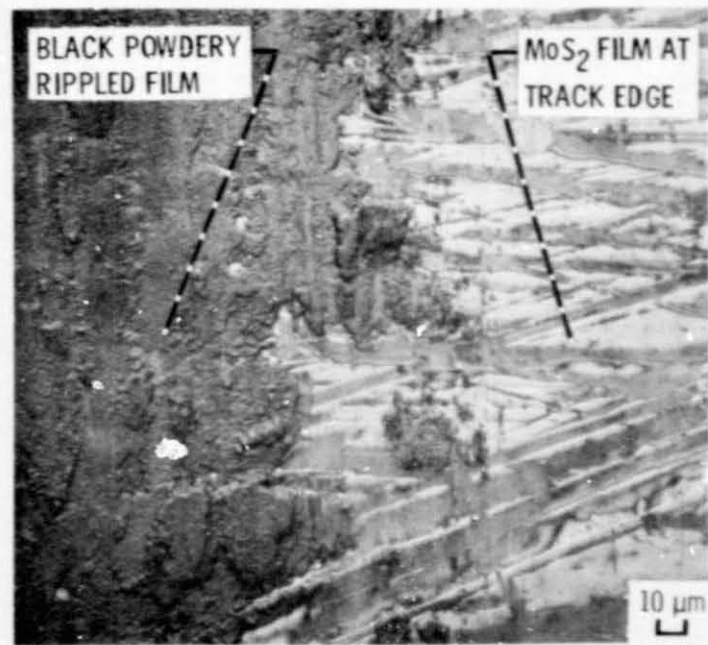
Figure 6. - Concluded.



(a) 1 kc OF SLIDING.



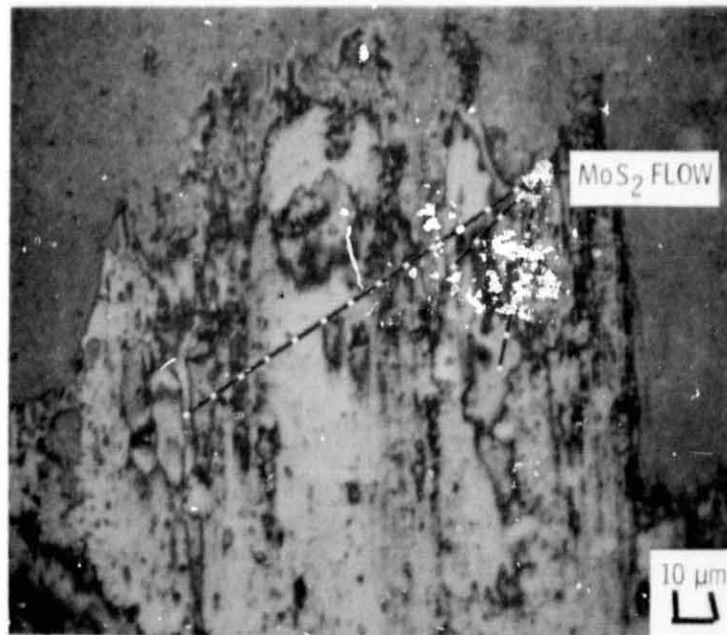
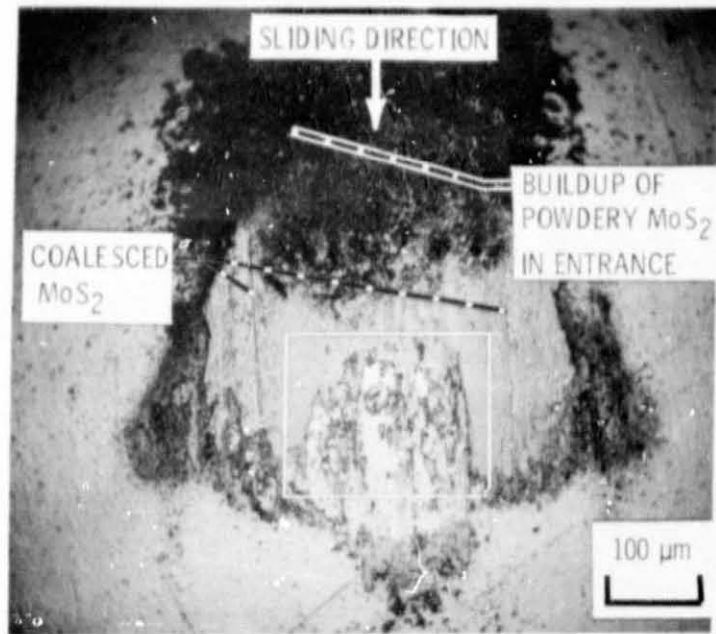
(b) 5 kc OF SLIDING.



(c) 10 kc OF SLIDING.

Figure 7. - High magnification photomicrographs of interesting features within the MoS<sub>2</sub> film wear tracks of figure 6.

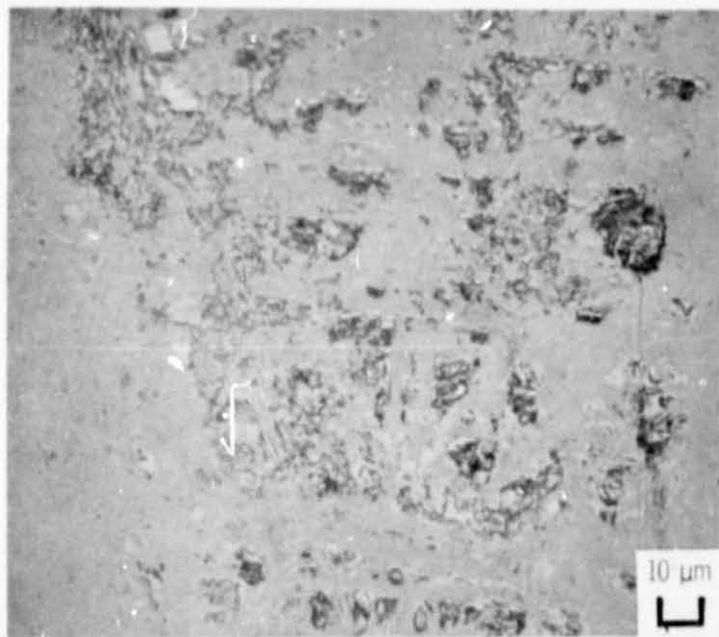
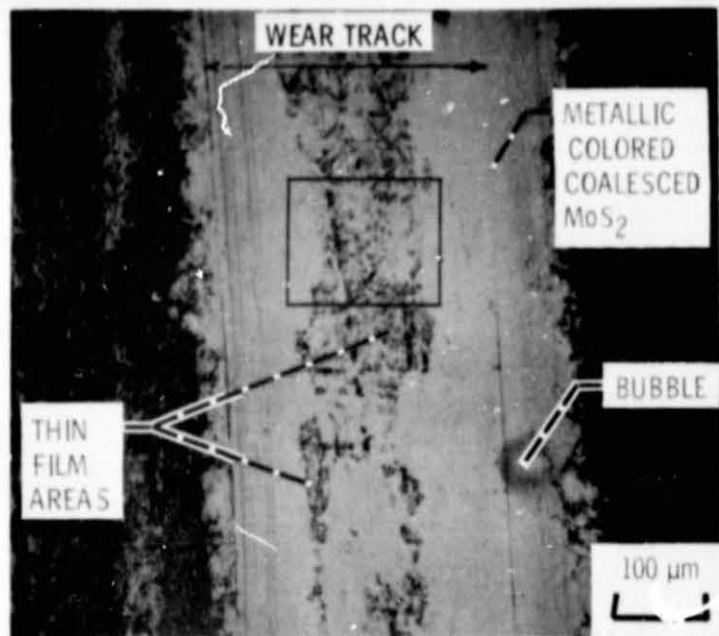
E-9633



(a) RIDER WEAR SCAR.

Figure 8. - Photomicrographs after sliding for 1 kilocycle in a dry air atmosphere (<20 ppm, H<sub>2</sub>O) at 25°C.

ORIGINAL PAGE IS  
OF POOR QUALITY

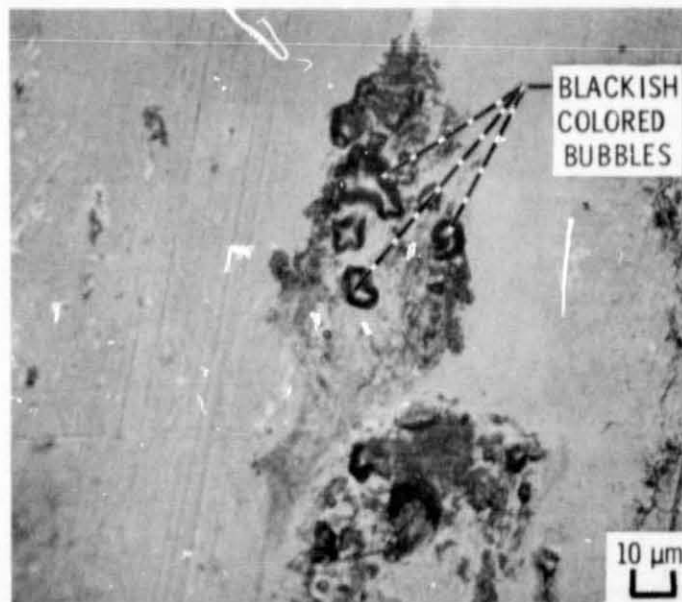
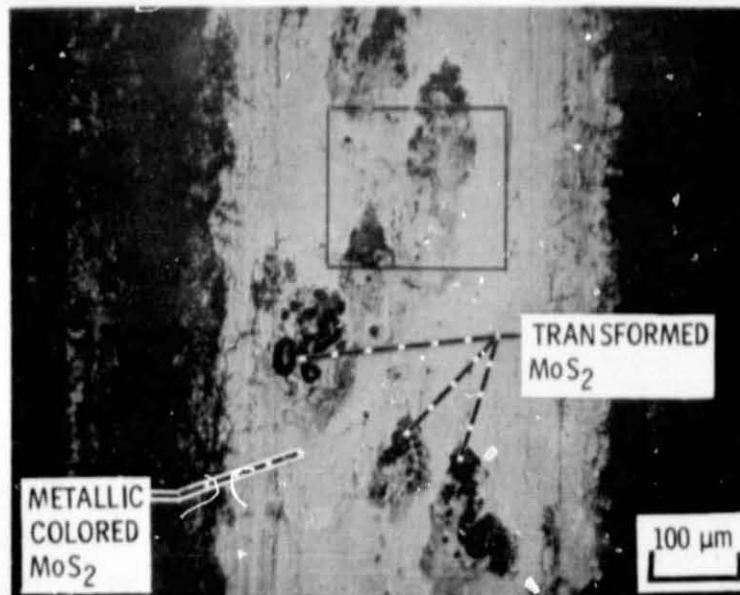


(b) MoS<sub>2</sub> FILM WEAR TRACK.

Figure 8. - Concluded.



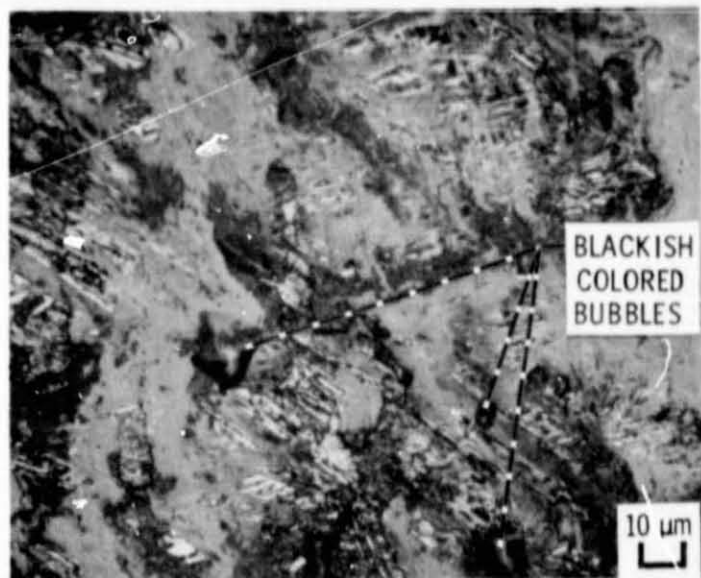
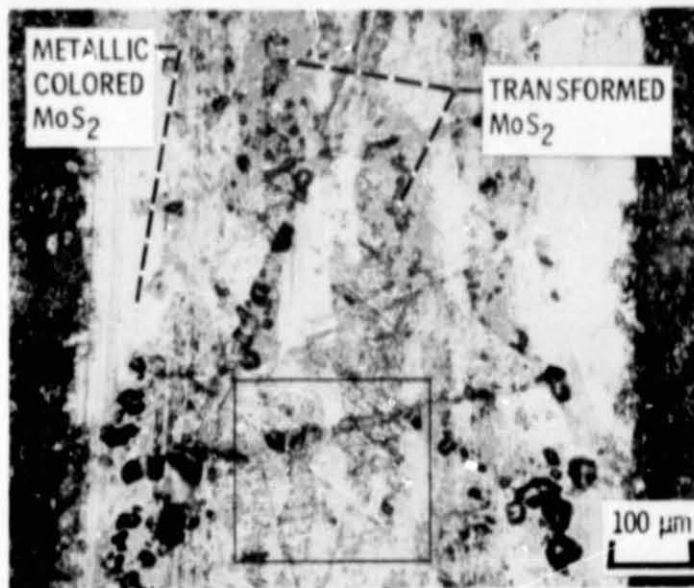
ORIGINAL PAGE IS  
OF POOR QUALITY



(a) 5 kc OF SLIDING.

Figure 9. - Photomicrographs of MoS<sub>2</sub> film wear tracks taken in a dry air atmosphere (<20 ppm H<sub>2</sub>O).

9633



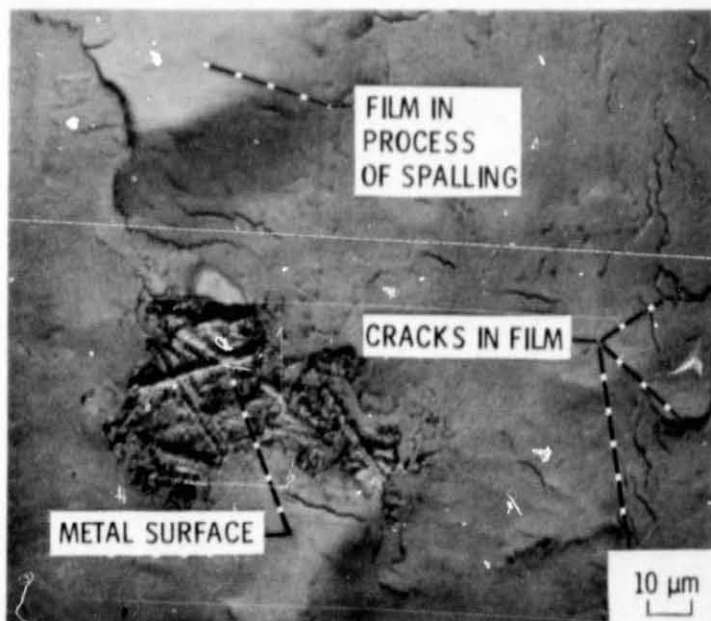
(b) 60 kc OF SLIDING.

Figure 9. - Concluded.

ORIGINAL PAGE IS  
OF POOR QUALITY



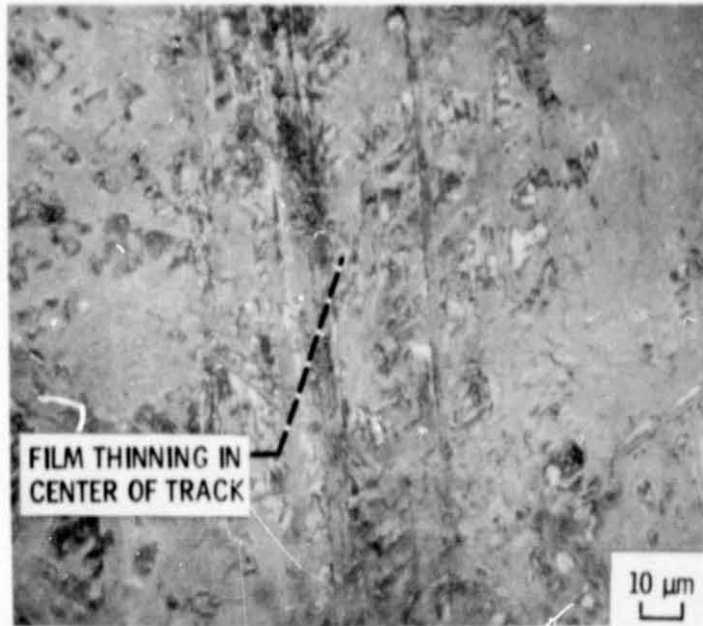
(a) 1 kc OF SLIDING.



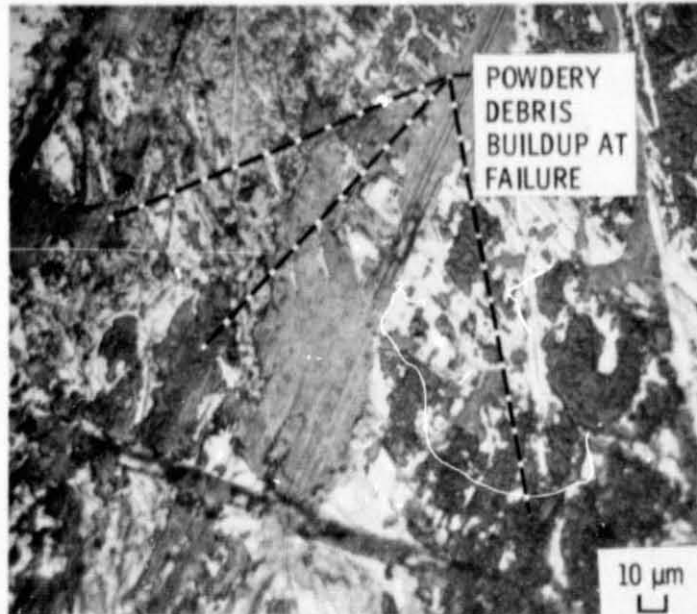
(b) 60 kc OF SLIDING.

Figure 10. - High magnification of MoS<sub>2</sub> film wear tracks which were obtained in a dry argon atmosphere (<20ppm H<sub>2</sub>O) after various sliding intervals.





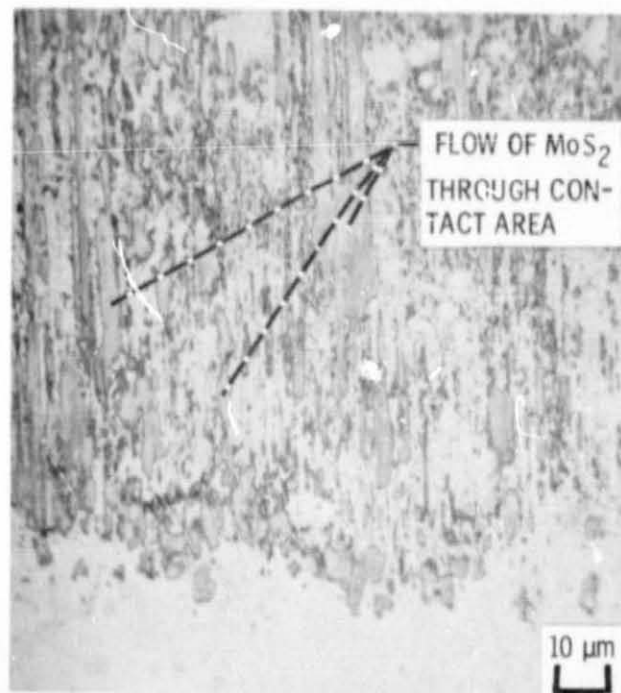
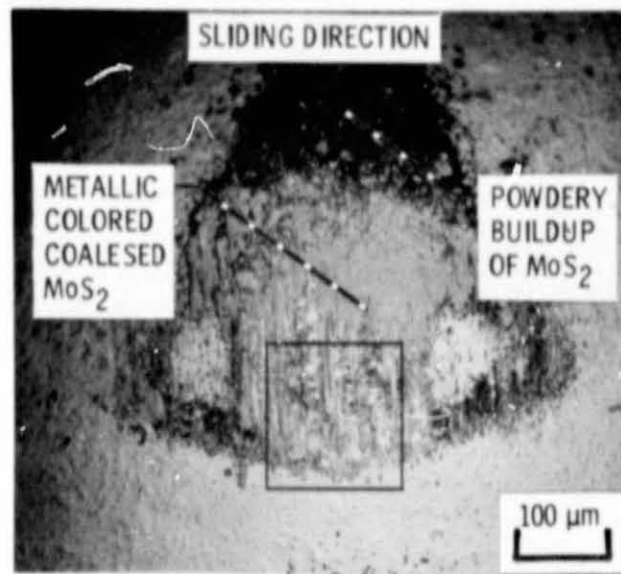
(c) 700 kc OF SLIDING.



(d) 1860 kc OF SLIDING.

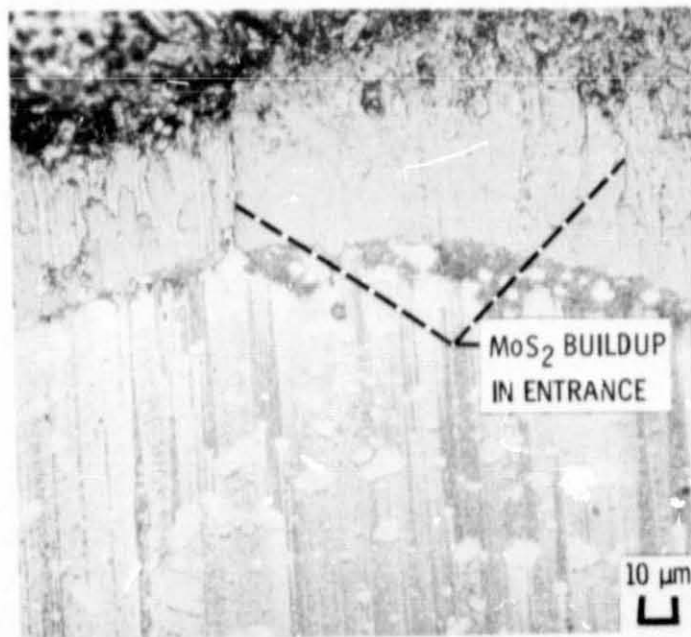
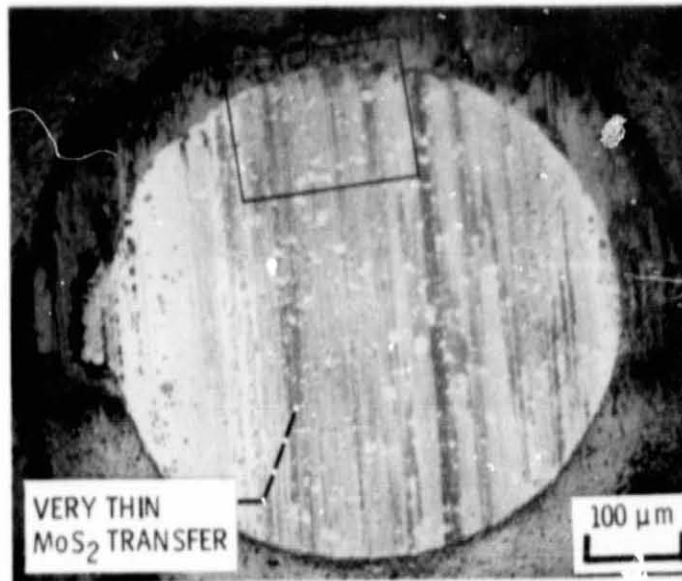
Figure 10. - Concluded.

ORIGINAL PAGE IS  
OF POOR QUALITY



(a) 1 kc OF SLIDING.

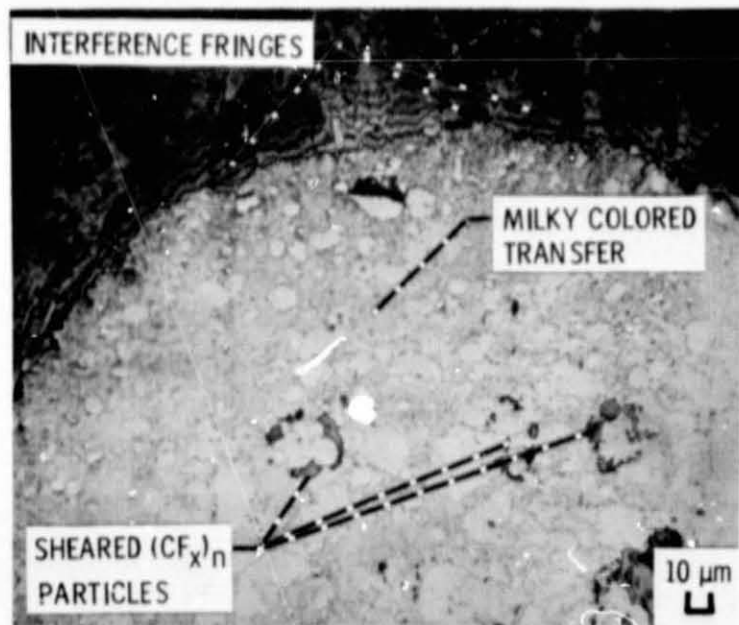
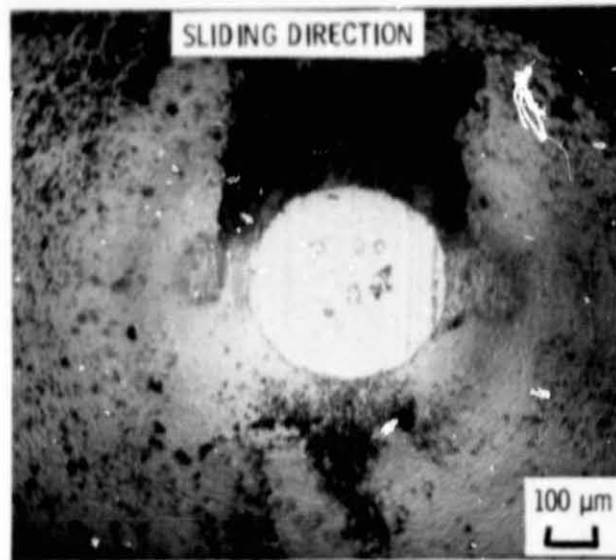
Figure 11. - Photomicrographs of MoS<sub>2</sub> rider transfer films in a dry argon atmosphere (<20 ppm H<sub>2</sub>O).



(b) 400 kc OF SLIDING.

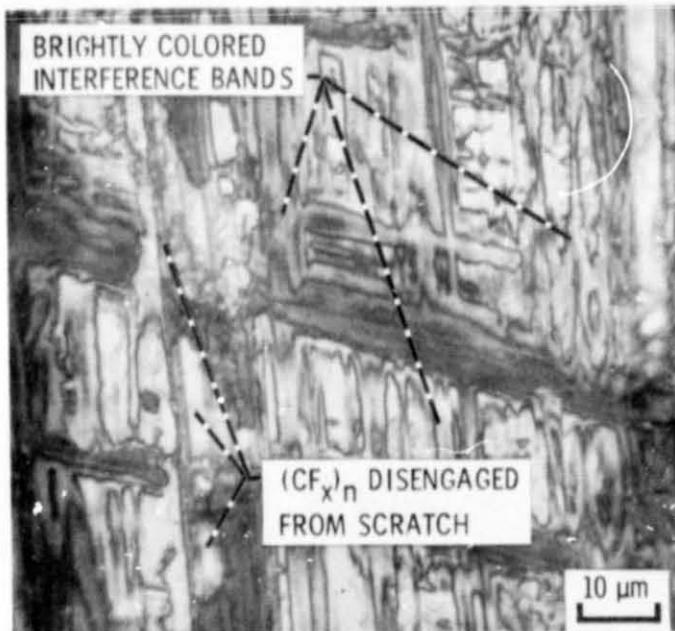
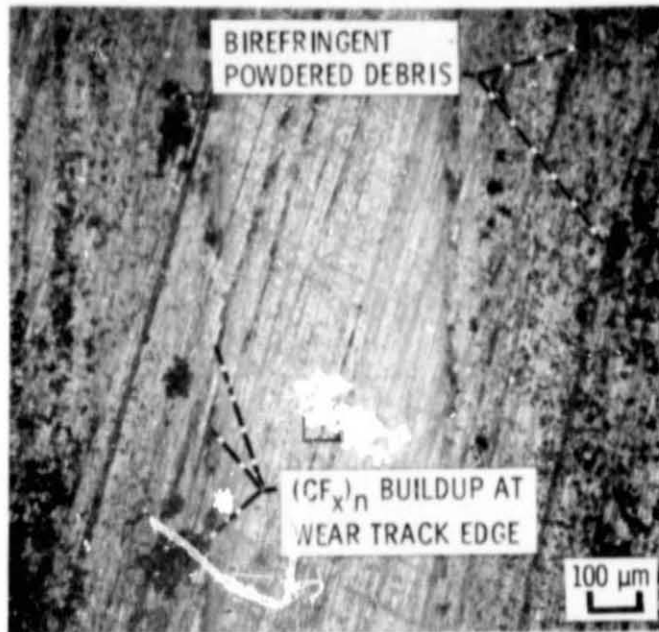
Figure 11. - Concluded.

ORIGINAL PAGE IS  
OF POOR QUALITY



(a) RIDER WEAR SCAR.

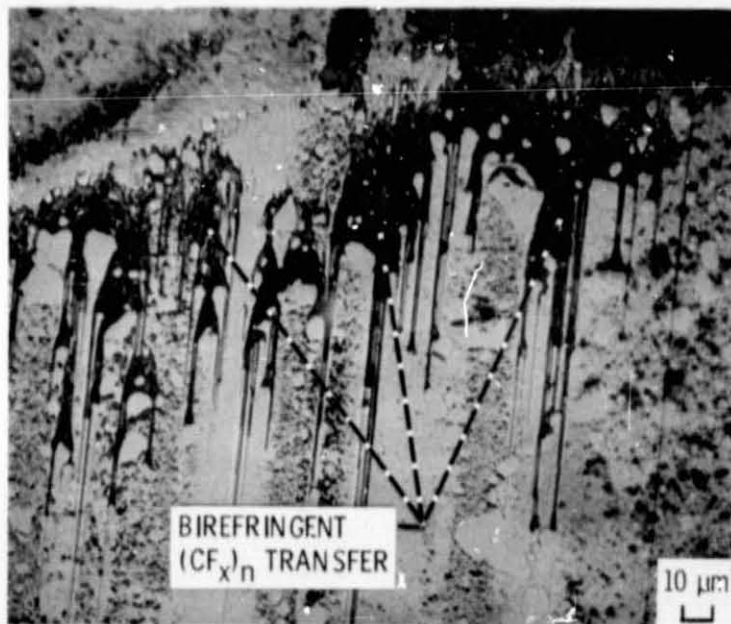
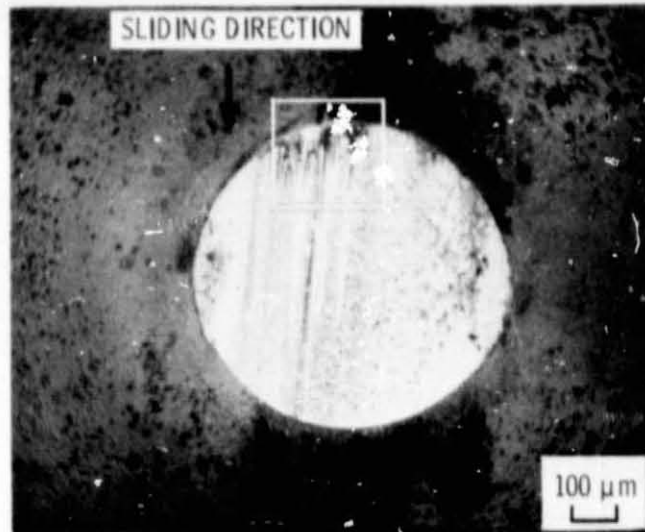
Figure 12. - Photomicrographs taken after 1 kilocycle of sliding in a moist air atmosphere (10 000 ppm  $\text{H}_2\text{O}$ ).



(b)  $CF_x$  FILM WEAR TRACK.

Figure 12. - Concluded.

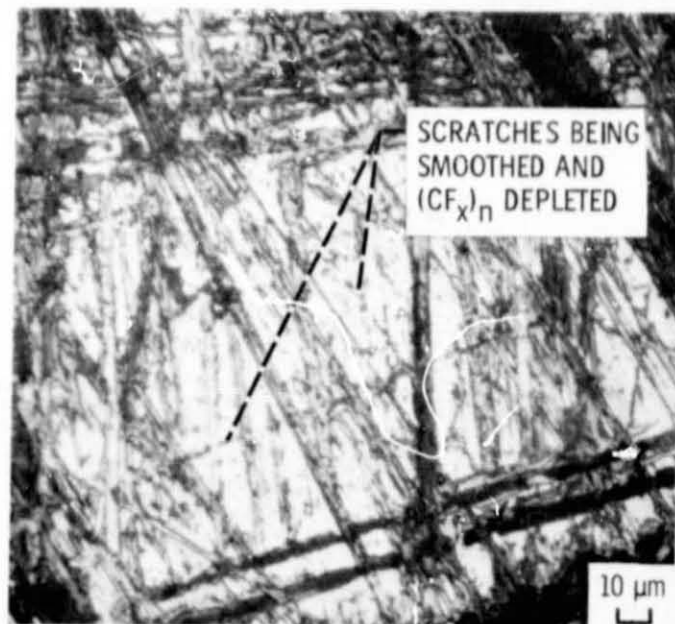
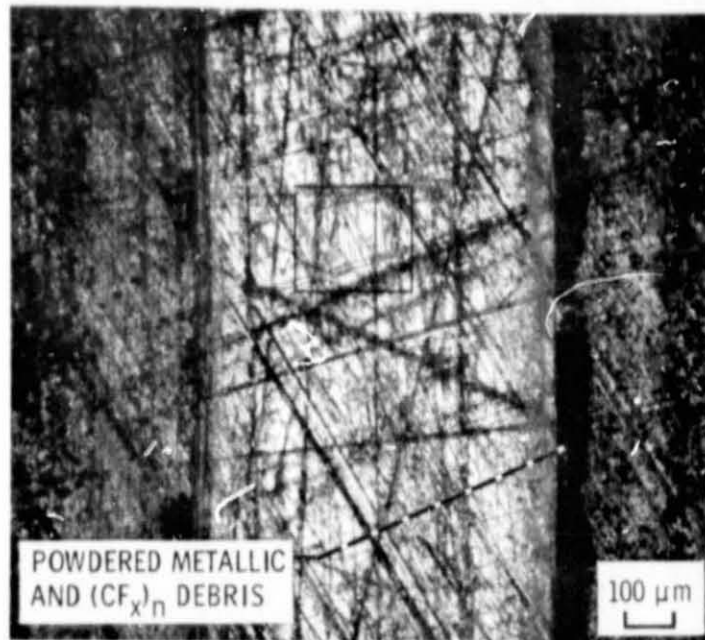
ORIGINAL PAGE IS  
OF POOR QUALITY



(a) RIDER WEAR SCAR.

Figure 13. - Photomicrographs taken after 100 kilocycles of sliding in a moist air atmosphere (10 000 ppm  $\text{H}_2\text{O}$ ).



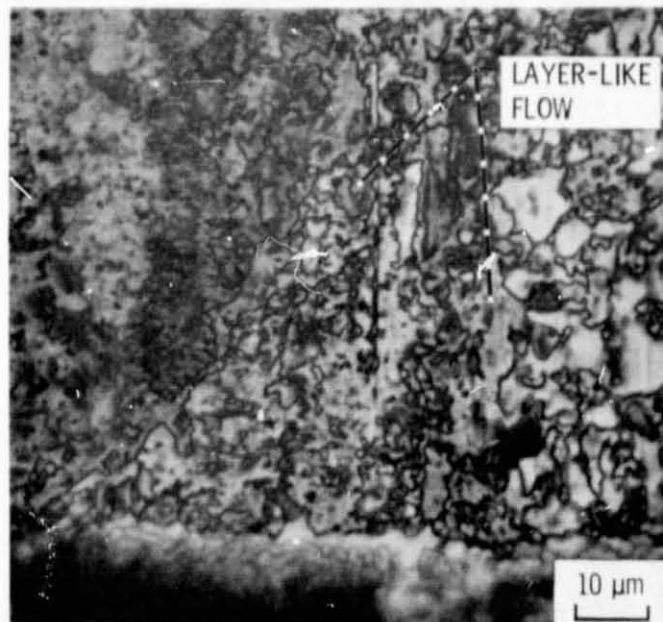
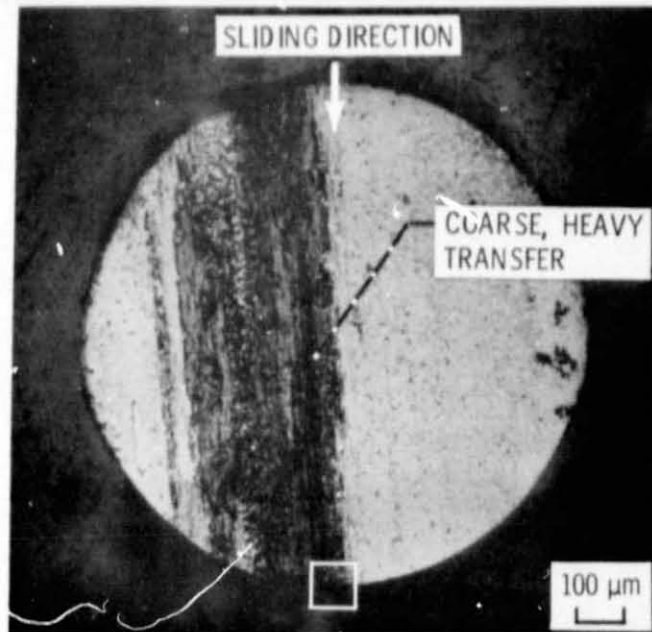


(b)  $(CF_x)_n$  FILM WEAR TRACK.

Figure 13. - Concluded.

ORIGINAL PAGE 16  
OF POOR QUALITY

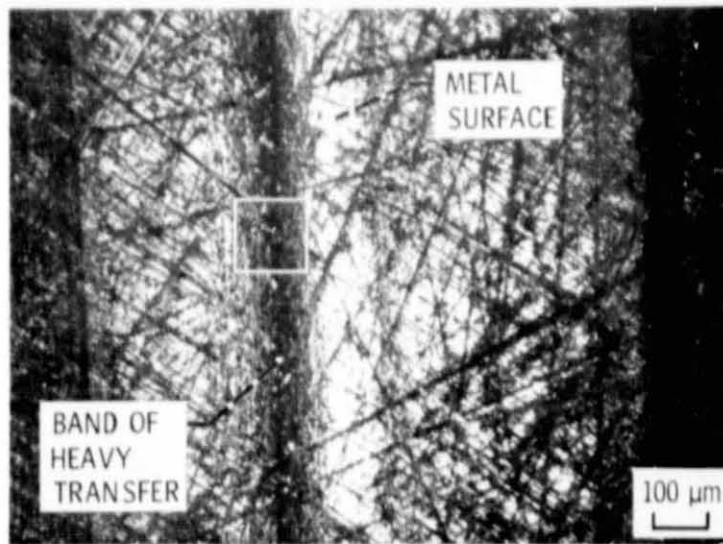
E-9633



(a) RIDER WEAR SCAR.

Figure 14. - Photomicrographs taken after 308 kilocycles of sliding in a moist air atmosphere (10 000 ppm H<sub>2</sub>O).

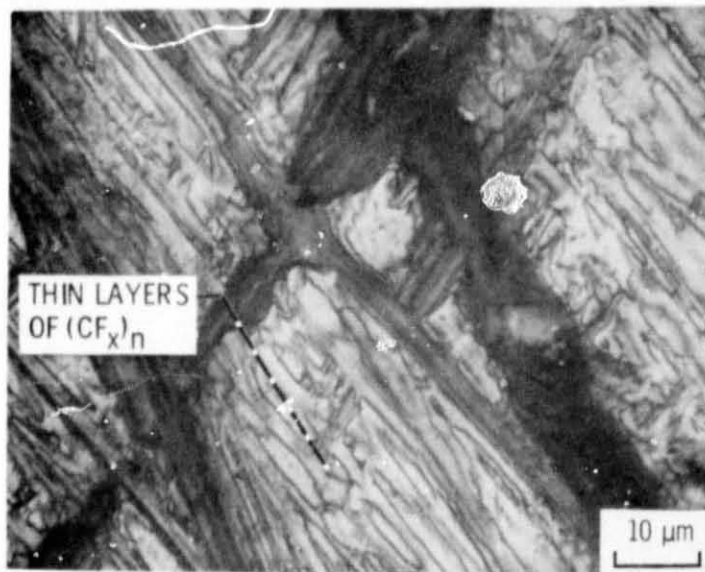
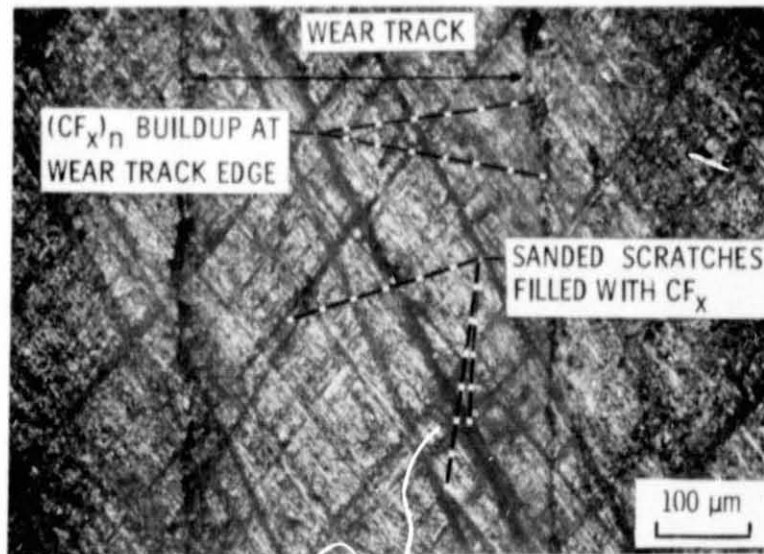




(b)  $(\text{CF}_x)_n$  FILM WEAR TRACK

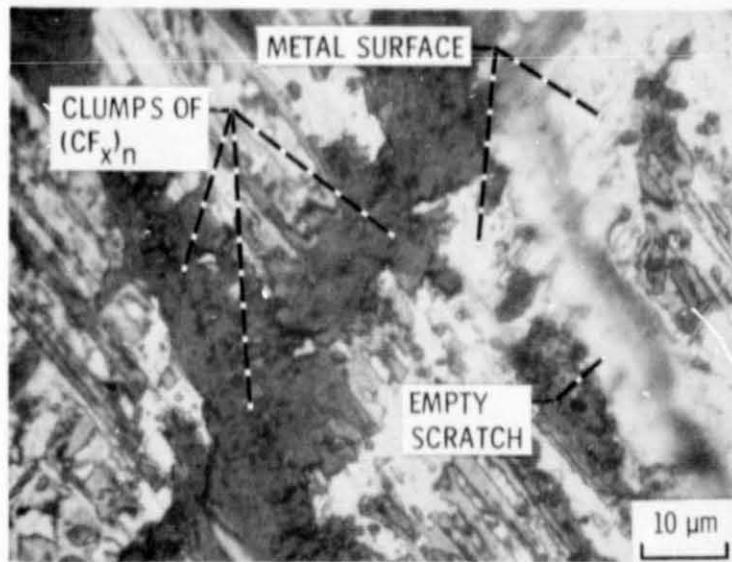
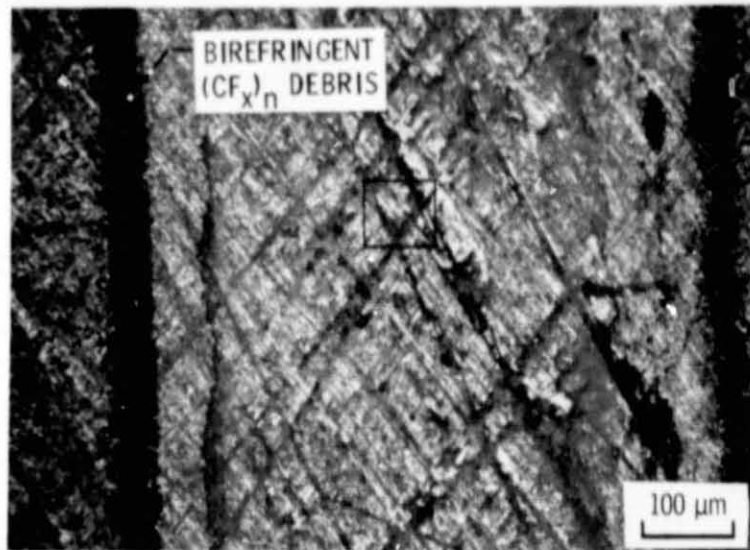
Figure 14. - Concluded.

ORIGINAL PAGE 16  
OF POOR QUALITY



(a) RUN-IN PHASE,  $\mu = 0.10$  (1/4 kc OF SLIDING).

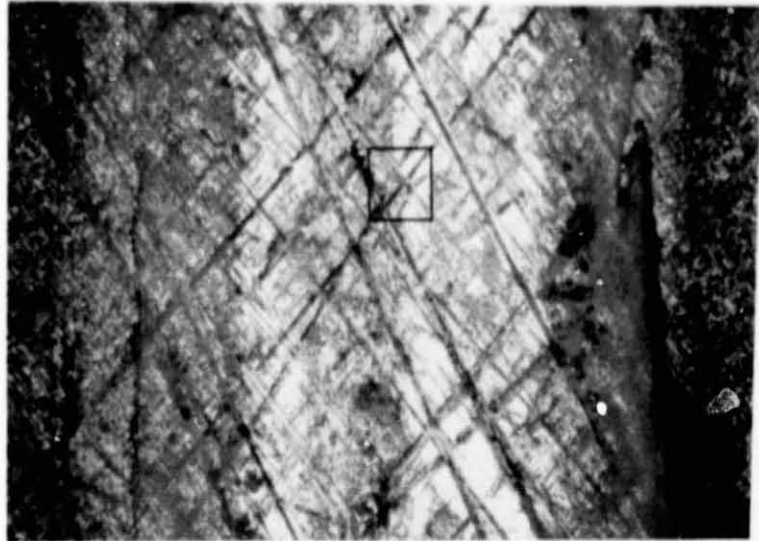
Figure 15. - Photomicrographs of the same area on a graphite fluoride film wear track after various sliding intervals in a dry air atmosphere ( $< 20$  ppm  $H_2O$ ).



(b) LOW FRICTION PHASE,  $\mu = 0.02$  (3 kc OF SLIDING).

Figure 15. - Continued.

ORIGINAL PAGE IS  
OF POOR QUALITY

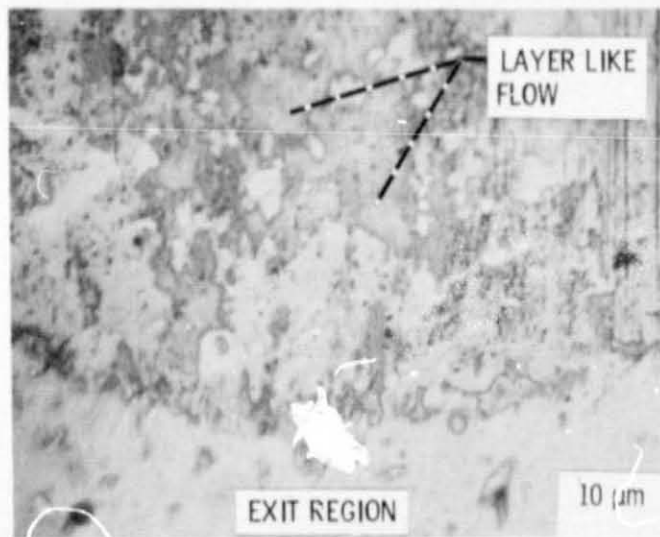
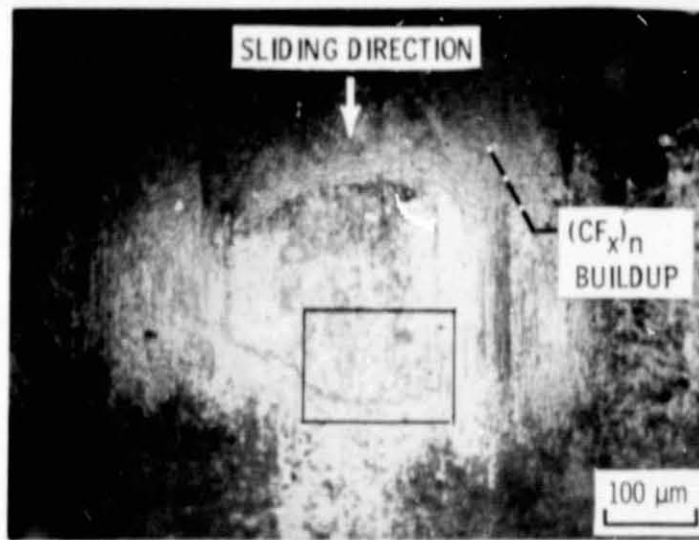


D-9633



(c) HIGH FRICTION PHASE,  $\mu = 0.20$  (24 kc OF SLIDING).

Figure 15. Concluded.

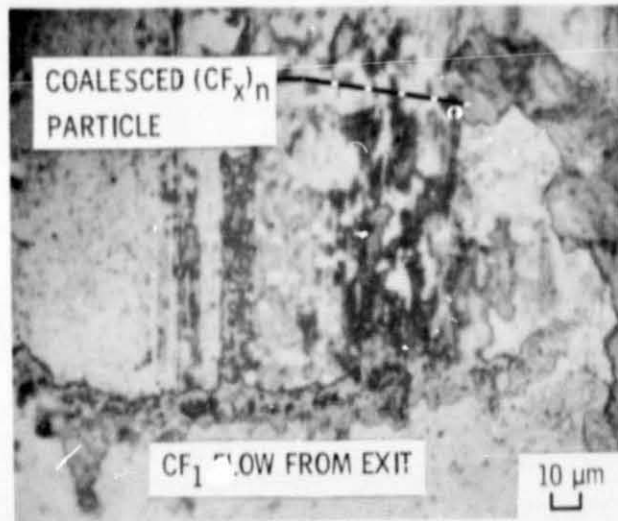
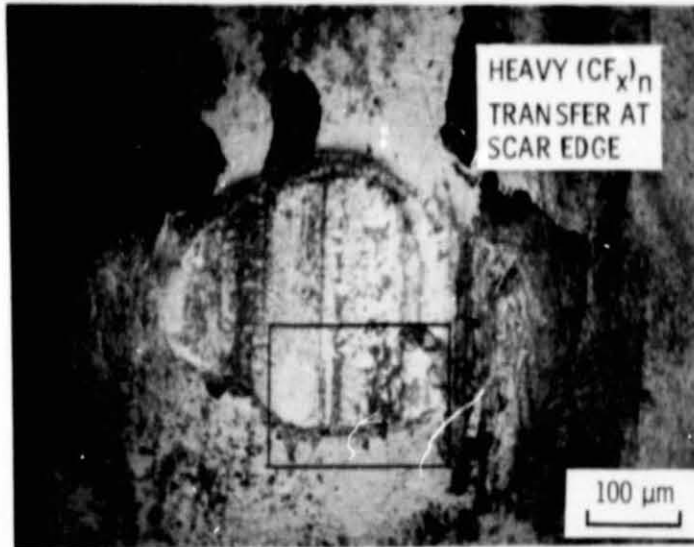


(a) RUN-IN PHASE,  $\mu = 0.10$  (1/4 kc OF SLIDING).

Figure 16. - Photomicrographs of rider wear scars which slid on the graphite fluoride films shown in figure 15.

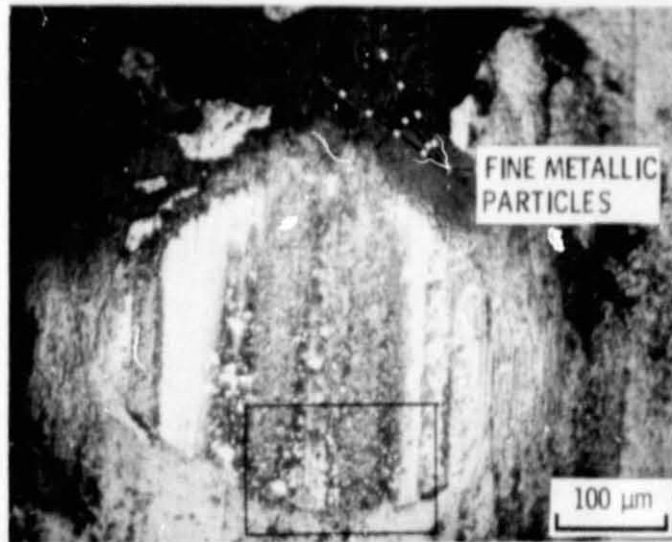


ORIGINAL PAGE IS  
OF POOR QUALITY



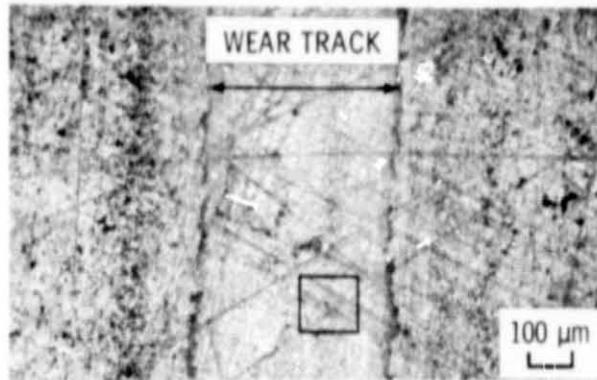
(b) LOW FRICTION PHASE,  $\mu = 0.02$  (3 kc OF SLIDING).

Figure 16. - Continued.



(c) HIGH FRICTION PHASE,  $\mu = 0.20$  (24 kc OF SLIDING).

Figure 16. - Concluded.



(a) 1kc OF SLIDING.

Figure 17. - Photomicrographs of a graphite fluoride film wear track after various sliding intervals in a dry argon atmosphere ( $< 20$  ppm  $H_2O$ ).

5-9633

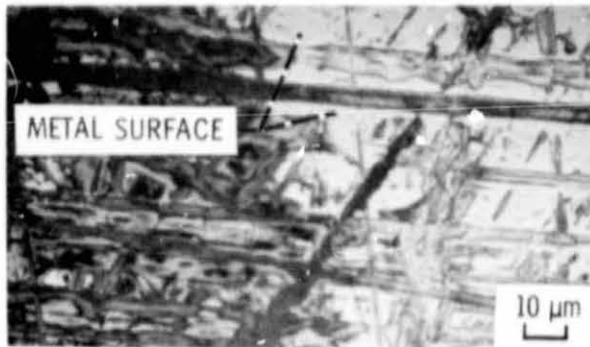
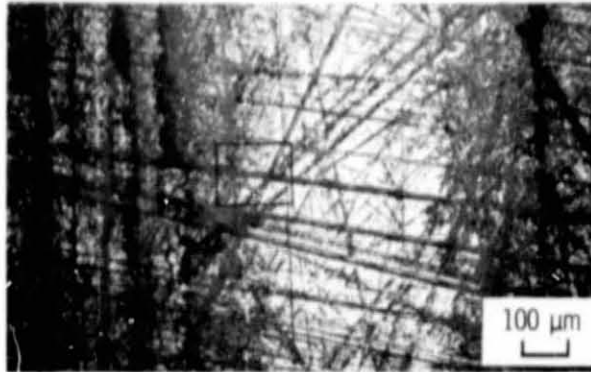




(b) 15 kc OF SLIDING.

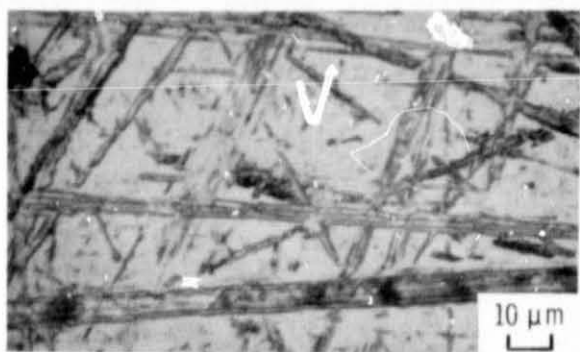
Figure 17. - Continued.

ORIGINAL PAGE IS  
OF POOR QUALITY



(c) 60 kc OF SLIDING.

Figure 17. - Continued.



(d) 180 kc OF SLIDING.

Figure 17. - Concluded.